α-1-C-Butyl-1,4-dideoxy-1,4-imino-L-arabinitol as a Second-Generation Iminosugar-Based Oral α-Glucosidase Inhibitor for Improving Postprandial Hyperglycemia

Atsushi Kato,*[†] Erina Hayashi,[†] Saori Miyauchi,[†] Isao Adachi,[†] Tatsushi Imahori,[‡] Yoshihiro Natori,[‡] Yuichi Yoshimura,[‡] Robert J. Nash,[§] Hideyuki Shimaoka,[∥] Izumi Nakagome,[⊥] Jun Koseki,[⊥] Shuichi Hirono,[⊥] and Hiroki Takahata*[‡]

[†]Department of Hospital Pharmacy, University of Toyama, Toyama 930-0194, Japan

[‡]Faculty of Pharmaceutical Sciences, Tohoku Pharmaceutical University, Sendai 981-8558, Japan

[§]Institute of Biological, Environmental and Rural Sciences/Phytoquest Limited, Plas Gogerddan, Aberystwyth, Ceredigion SY23 3EB, United Kingdom

[∥]S-BIO Business Division, Simitomo Bakelite Company Limited, Tokyo 140-0002, Japan

[⊥]School of Pharmaceutical Sciences, Kitasato University, Tokyo 108-8641, Japan

Ⓢ Supporting Information

ABSTRACT: We report on the synthesis and the biological evaluation of a series of α-1-C-alkylated 1,4-dideoxy-1,4-imino-L-arabinitol (LAB) derivatives. The asymmetric synthesis of the derivatives was achieved by asymmetric allylic alkylation, ring-closing metathesis, and Negishi cross-coupling as key reactions. α-1-C-Butyl-LAB is a potent inhibitor of intestinal maltase, isomaltase, and sucrase, with IC_{50} values of 0.13, 4.7, and 0.032 μM, respectively. Matrix-assisted laser desorption ionization time-of-flight mass spectrometric analysis revealed that this compound differs from miglitol in that it does not influence oligosaccharide processing and the maturation of glycoproteins. A molecular docking study of maltase-glucoamylase suggested that the interaction modes and the orientations of α-1-C-butyl-LAB and miglitol are clearly different. Furthermore, α-1-C-butyl-LAB strongly suppressed postprandial hyperglycemia at an early phase, similar to miglitol in vivo. It is noteworthy that the effective dose was about 10-fold lower than that for miglitol. α-1-C-Butyl-LAB therefore represents a new class of promising compounds that can improve postprandial hyperglycemia.
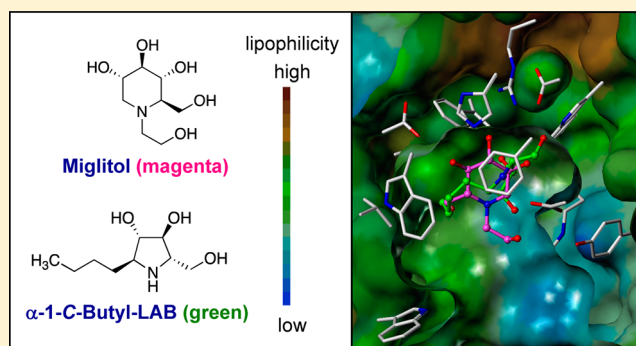
INTRODUCTION

Diabetes mellitus, one of the most common chronic metabolic diseases, occurs when the pancreas produces insufficient levels of insulin, or when the body cannot effectively use the insulin it produces.[1-3] Type 2 diabetes is induced by a combination of factors, including lifestyle and genetic factors. Today, the worldwide prevalence of diabetes is taking on pandemic dimensions, as changing lifestyles lead to reduced physical activity and increased obesity. In 2010, 285 million people were suffering from diabetes, and this number is estimated to increase to 439 million by 2030.[4] In recent years, it has been proposed that acute blood glucose elevations induce vascular damage through direct action on the vascular endothelium and finally cause myocardial infarctions, coronary heart disease, and cerebral apoplexy.[5] Therefore, the careful control of blood glucose levels can delay or protect at-risk subjects from developing cardiovascular diseases.[6-9] Antidiabetic drugs are currently classified into several different mechanistic classes (e.g., insulin secretagogues such as sulfonylureas, insulin

sensitizers such as biguanides and thiazolidinediones, insulin mimetics such as glucagon-like peptide analogues and agonists, α-glucosidase inhibitors, and DPP IV inhibitors). However, some of these drugs have unacceptable side effects in some patients or lose their effectiveness over time. Therefore, the search for new antidiabetic drugs has continued to attract considerable interest.

Among these drugs, α-glucosidase inhibitors are oral antidiabetic agents which suppress postprandial hyperglycemia by inhibiting the hydrolysis of disaccharides such as maltose, isomaltase, and sucrose in the brush border membrane and delaying the absorption of carbohydrates from the small intestine. A recent metaregression analysis revealed that a close relationship exists between 2 h postprandial glucose levels and cardiovascular risk below the diabetic threshold,[10] and there is growing epidemiological evidence to show that an association

between postprandial hyperglycemia and macrovascular complications exists in diabetic individuals.[11−13] Therefore, α-glucosidase inhibitors have considerable potential for preventing these cardiovascular risks. At present, a large number of compounds mimicking the structures of monosaccharides or oligosaccharides have been discovered from natural sources, which include thiosugars.[14−16] Among them, N-containing α-glucosidase inhibitors belong to two different main chemical classes. The first class is carbasugar-based inhibitors such as acarbose and voglibose. Carbasugars are carbocyclic analogues of hexopyranoses in which the ring oxygen has been replaced by carbon.[17] 5a-Carba-α-D-glucopyranosylamines such as validamine,[18] valienamine,[19] and valiolamine[20] in particular have proved to be important lead compounds for the development of clinically important antidiabetic agents. The first commercially available antidiabetic α-glucosidase inhibitor acarbose was introduced into the market in Germany in 1990 and has since been successfully marketed in Europe and Latin America. Voglibose was designed from valiolamine. It was produced by the reductive amination of valiolamine with dihydroxyacetone and was intended to function as an oral antidiabetic agent.[21] The second class of α-glucosidase inhibitors is iminosugar-based inhibitors such as miglitol. Iminosugars are sugar mimics with a nitrogen atom in place of the ring oxygen of monosaccharides. Miglitol was designed from 1-deoxynojirimycin (DNJ). DNJ has an excellent α-glucosidase inhibitory activity in vitro,[22] whereas its efficacy in vivo is only moderate.[23] Therefore, a large number of DNJ derivatives have been prepared in the hopes of increasing in vivo activity for this class of compounds.[24−26] Finally, N-(hydroxyethyl)-DNJ (miglitol) was reported to be the most favorable inhibitor out of a large number of in vitro active agents, and it was introduced into the market in 1999 as a more potent second-generation α-glucosidase inhibitor.

Although the mechanisms of action against intestinal enzymes for these two classes of α-glucosidase inhibitors are similar, each has a distinct clinical strategy. The most important arguing point is whether absorption from the intestinal tract is of benefit to the clinical effects. Glycosidases, which are involved in several important anabolic and catabolic processes, act not only on intestinal digestion but also on lysosomal catabolism and the post-translational modification of glycoproteins. The inhibition of liver and lysosomal glycosidases is occasionally responsible for the development of serious hepatic dysfunctions.[27] Thus, carbasugar-based drugs were designed to not cross the intestinal membranes. Acarbose is poorly absorbed from the gastrointestinal tract, the mean systemic bioavailability being only between 0.5% and 1.6%.[28] Similarly, voglibose is designed with a propanediol group from valiolamine for the purpose of disrupting its absorption. However, this poor absorption means that the drug stays in the intestine and colon for a long period of time and is associated with a high frequency of side effects such as flatulence, diarrhea, and hypoglycemia. In contrast, the iminosugar-based drug miglitol was designed to be nearly completely absorbed from the intestinal tract and may possess systemic effects in addition to affecting the intestinal border.[29,30] Previous experiments showed that the plasma half-life of miglitol is 2.4 h with a plasma peak concentration of 1.1 mg/L and a peak T_{max} of 2.3 h after an oral administration of 2 mg/kg of body weight.[31] Moreover, these studies revealed that there are two different glucose suppression mechanisms associated with miglitol, both direct and indirect. It directly and reversibly inhibits the α-

glucosidase enzyme, and it induces the secretion of the glucagon-like peptide-1 (GLP-1). GLP-1 is a gut incretin hormone that is considered to be a promising therapeutic agent for type 2 diabetes because it stimulates β-cell proliferation, insulin secretion, and sensitivity in a glucose-dependent manner.[32,33] However, this absorption activity invites the risk of potential hepatic dysfunction.

Thus, our strategy has been to design effective iminosugar-type α-glucosidase inhibitors that affect postprandial hyperglycemia that not only show strong inhibitory effects against maltase, isomaltase, and sucrase but also do not interfere with the processing of glycoproteins. As part of our research program aimed at developing new potent and selective α-glucosidase inhibitors, we reported that the synthetic enantiomer 1,4-dideoxy-1,4-imino-L-arabinitol (LAB) is a more active and selective inhibitor of α-glucosidases than the natural product 1,4-dideoxy-1,4-imino-D-arabinitol (DAB).[34] In addition, the introduction of a branched carbon chain at the C4 position led to an improved sucrase inhibition (IC$_{50}$ = 0.66 μM).[35] Considering this remarkable activity, we envisaged that a further improvement in activity might be gained in the case of structures having a longer side chain. To test this hypothesis, a series of α-1-C-alkylated LAB derivatives were then prepared by asymmetric allylic alkylation (AAA), ring-closing metathesis (RCM), and Negishi cross-coupling as key reactions. We herein describe the synthesis and biological evaluation of a series of α-1-C-alkylated LAB derivatives, which includes their suppressive effects on blood glucose levels using a carbohydrate loading test and their effects on whole cell glycoproteins, as determined by matrix-assisted laser desorption ionization time-of-flight mass spectrometric (MALDI-TOF MS) analysis. We also studied the selectivity of α-1-C-butyl-LAB for intestinal α-glucosidases vs intestinal β-glycosidases and lysosomal β-glucocerebrosidase. An additional aim was to demonstrate the molecular docking properties of α-1-C-butyl-LAB with maltase with the intention of determining the extent of difference from miglitol.

■ CHEMISTRY

Initially, the bicyclic 2,5-dihydropyrrole **2** was selected as the common intermediate for the synthesis of **1a−l** (Scheme 1).[36] The iodide **2** was prepared by iodination of oxazolidinol **3**, obtained by a modified Trost procedure.[37] With the iodide **2** in hand, Csp³−Csp³ bond formation using metal-catalyzed cross-

Scheme 1. Synthesis of α-l-C-Alkyl-LAB[a]
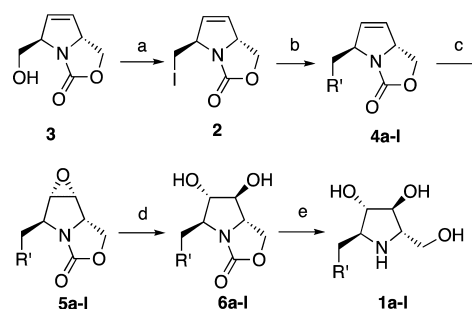
[a]Reagents: (a) I$_2$, Ph$_3$P, imidazole, CH$_2$Cl$_2$; (b) bis(l,5-cyclooctadiene)nickel(0), (S,S)-2,6-bis(4-isopropyl-2-oxazolin-2-yl)-pyridine, then alkylzinc bromide, N,N-dimethylacetamide; (c) ethylenediaminetetraacetic acid, 1,1,1-trifluoroacetone, Oxone, NaHCO$_3$, CH$_3$CN, H$_2$O; (d) trifluoroacetic acid, THF/H$_2$O; (e) NaOH, EtOH/H$_2$O.

coupling was examined owing to homologation of the alkyl substituents. Among the several procedures examined, the Negishi cross-coupling reaction developed by Fu et al.[38,39] was successful and gave the desired alkyl-substituted oxazolidinones **4a–l** (Table 1). The epoxidation of olefin in **4a–l** with the

Table 1. Negishi Cross-Coupling of 2 with Alkylzinc Halides Using Catalytic Ni(COD)$_2$ in the Presence of a Tridentate Nitrogen Ligand [(R,R)-i-Pr-Pybox]

entry	R′ZnX	product	yield[a] (%)
1	MeZnI	**4a**	69
2	EtZnI	**4b**	63
3	n-PrZnBr	**4c**	78
4	n-BuZnBr	**4d**	63
5	n-C$_5$H$_{11}$ZnBr	**4e**	69
6	n-C$_6$H$_{13}$ZnBr	**4f**	69
7	n-C$_7$H$_{15}$ZnBr	**4g**	68
8	n-C$_8$H$_{17}$ZnBr	**4h**	72
9	n-C$_9$H$_{19}$ZnBr	**4i**	66
10	n-C$_{10}$H$_{21}$ZnBr	**4j**	71
11	Ph(CH$_2$)$_3$ZnBr	**4k**	73
12	(CH$_3$)$_2$CH(CH$_2$)$_2$ZnBr	**4l**	76

[a]Isolated yield.

dioxirane, generated in situ from Oxone with 1,1,1-trifluoroacetone, resulted in the stereoselective formation of epoxides **5a–l**. Since the alkyl substituents of **4** are oriented toward the axial position of an approximate planar bicycloxazolone in a molecular model, the stereochemistry of the epoxide was deduced to be *anti* with respect to the alkyl substituents. Ring-opening of the epoxide with aqueous TFA stereoselectively proceeded to provide diols **6a–l**. The stereochemistries of diols of **6c** were determined to be 6α and 7β configurations, because an NOE correlation was observed between the hydrogen at C-5 and the hydrogen at C-7. Finally, the oxazolinones **6a–l** were transformed by basic hydrolysis into the desired iminosugars **1a–l** (Table 2).[40]

Table 2. Yields of the Three-Step Sequence from 4 to 1

| entry	R′	product	yield[a] (%)
1	Me	**1a**	51
2	Et	**1b**	58
3	n-Pr	**1c**	43
4	n-Bu	**1d**	52
5	n-C$_5$H$_{11}$	**1e**	55
6	n-C$_6$H$_{13}$	**1f**	59
7	n-C$_7$H$_{15}$	**1g**	35
8	n-C$_8$H$_{17}$	**1h**	49
9	n-C$_9$H$_{19}$	**1i**	30
10	n-C$_{10}$H$_{21}$	**1j**	45
11	Ph(CH$_2$)$_3$	**1k**	55
12	(CH$_3$)$_2$CH(CH$_2$)$_2$	**1l**	62

[a]Isolated yield.

Next the tetrols **7** and **8** were prepared from an enantiomer (2R,5R configuration), **9**, of the known *ent*-**9**,[34] as shown in Scheme 2. Treatment of the Weinreb amide **9** with propylmagnesium bromide gave the ketone **10** in 78% yield, which was reduced with DIBAL-H to afford the β-alcohol **11** and the α-alcohol **12** in a ratio of 4:1. On the other hand, the reduction of **10** with NaBH$_4$ provided **12** and **11** in a 2:1 ratio

with inverse selectivity. These selectivities were previously observed in a similar example by Trost et al.[37] Epoxidation of **11** included the relative amount of two epoxides, **13**, which were cleaved by hydrolysis to give the same triol **14** as a single diastereomer. Probably, S$_N$2 attack of water occurs from the sterically less hindered side of both epoxides to produce the same product **14**.[34] Finally, hydrogenolysis of **14** afforded the desired tetrol **7**. Similarly, **12** was transformed via **15** and **16** into **8**.

In addition, the N-butyl derivative **17** of **1c** and compound **18** with a 3-butyl substituent in place of the 3-hydroxy of **1c** were prepared as exhibited in Scheme 3. Reductive amino alkylation of **1c** with butyraldehyde in the presence of NaBH$_3$CN gave N-butyl-1-C-butyl-LAB (**17**). Next the epoxide of **5c** was cleaved by n-butyllithium in the presence of CuI to provide **19**, which was hydrolyzed with base to give 1,3-C-dibutyl-LAB (**18**).

BIOLOGICAL RESULTS AND DISCUSSION

Evaluation of N- or 1-C-Butyl-LAB and -DNJ Derivatives as Glycosidase Inhibitors. In connection with our recent work concerning the synthesis of pyrrolidine-based iminosugars with a branched carbon chain of biological interest,[35,41] we turned our attention to the design of potent and selective α-glucosidase inhibitors with the goal of reducing postprandial hyperglycemia. We first evaluated N-butyl-LAB and α-1-C-butyl-LAB, since a previous structure−activity relationship study indicated that the natural product DAB is a good inhibitor, but the enantiomer LAB is a more potent inhibitor of α-glucosidases.[42] N-Butyl-1-deoxynojirimycin (N-butyl-DNJ) and α-1-C-butyl-DNJ were also tested to extend our understanding of the effect of introducing an alkyl substituent into an iminosugar. We found that the inhibitory potency of the parent DNJ was slightly better than that of LAB against α-glucosidases (Table 3). However, DNJ showed a broad inhibition spectrum against β-glucosidases, β-galactosidases, and trehalases. The introduction of an N-butyl substituent into LAB and DNJ reduced their effectiveness as glycosidase inhibitors. In sharp contrast, the introduction of a butyl chain at C-1 of LAB to give α-1-C-butyl-LAB dramatically improved its inhibitory potency against sucrase, with an IC$_{50}$ value of 0.032 μM. We were also intrigued by the fact that α-1-C-butyl-LAB showed no significant inhibition toward liver and lysosomal β-glucosidases and β-galactosidases, even at a concentration of 1000 μM. α-1-C-Butyl-DNJ was a potent inhibitor of isomaltase, whereas this compound was also a good inhibitor of human lysosome β-glucocerebrosidase, with an IC$_{50}$ value of 70 μM. Previous reports pointed out that these nonspecific inhibitions may cause undesirable side effects in the treatment of diabetes. In sharp contrast, α-1-C-butyl-LAB showed no significant inhibition toward β-glucocerebrosidase. To clarify the structural basis of the interaction of α-1-C-butyl-DNJ and α-1-C-butyl-LAB with human β-glucocerebrosidase, we constructed three-dimensional structures of the human β-glucocerebrosidase complexed with α-1-C-butyl-LAB or α-1-C-butyl-DNJ. As shown in Figure 1, α-1-C-butyl-DNJ and α-1-C-butyl-LAB were found to bind to β-glucocerebrosidase with the same orientation. Both α-1-C-butyl-DNJ and α-1-C-butyl-LAB interacted with aromatic groups such as Tyr313 and Phe246. However, the estimated binding energy (ΔE) of α-1-C-butyl-DNJ (−219.08 kcal mol^{-1}) with β-glucocerebrosidase indicated that it was more stable than 1-C-butyl-LAB (−185.87 kcal mol^{-1}) (Table 4). These differences (ΔΔE) in binding energies

Scheme 2. Synthesis of 7 and 8[a]
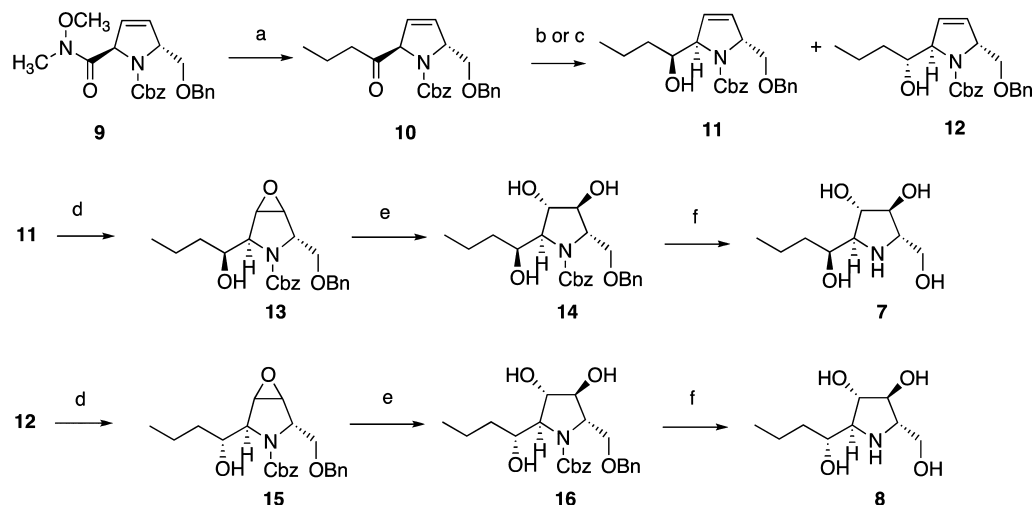
[a]Reagents: (a) PrMgBr, THF, 78%; (b) DIBAL-H, Et$_2$O, 65% for **11**, 18% for **12**; (c) NaBH$_4$, MeOH, 24% for **11**, 51% for **12**; (d) ethylenediaminetetraacetic acid, 1,1,1-trifluoroacetone, Oxone, NaHCO$_3$, CH$_3$CN, H$_2$O, 83% for **13**, 80% for **15**; (e) trifluoroacetic acid, THF/H$_2$O, 93% for **14**, 16% for **16**; (f) H$_2$, 5% Pd−C, concd HC1, MeOH, 68% for **7**, 94% for **8**.

Scheme 3. Synthesis of 17 and 18[a]
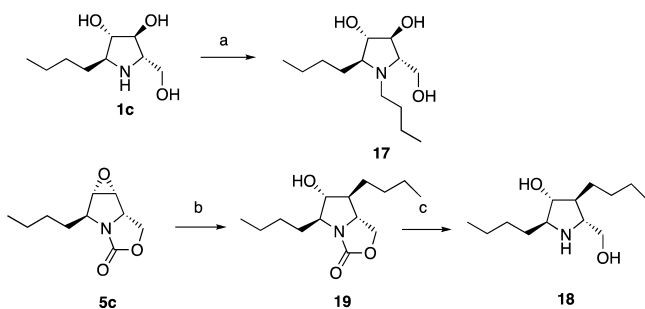
[a]Reagents: (a) NaBH$_3$CN, butyraldehyde, CH$_3$OH, 46%; (b) CuI, Et$_2$O, then n-BuLi, n-hexane, 23%; (c) NaOH, EtOH/H$_2$O, 38%.

may explain the differences in inhibition potency against β-glucocerebrosidase.

Optimization of the α-1-C-Alkyl Chain Length. On the basis of these findings, it clearly appeared that the addition of an alkyl chain at C-1 of LAB might lead to the production of highly potent and selective inhibitors of intestinal maltase and sucrase. Thus, we focused on the anomeric position and whether extending the alkyl chain at this position could influence the inhibition activities of LAB (Figure 2). Of these compounds, the introduction of short (ethyl and propyl) and longer (decyl and undecyl) groups reduced the inhibition activities compared to that of LAB (Table 5). Furthermore, we found that the inhibitory potency of α-1-C-alkyl-LAB against isomaltase derivatives decreased with increasing length of the alkyl chain. There is, therefore, a minimum 1-C-alkyl chain length requirement for achieving a strong inhibition of maltase and sucrase, with a butyl group being optimal. To check if the change from LAB to DNJ in the iminosugar part had an influence on activity toward intestinal α-glucosidases, we prepared α-1-C-alkyl-DNJs **19**−**21**. This comparison revealed that the inhibitory activity of α-1-C-alkyl-DNJs against maltase and sucrase was even weaker than that of α-1-C-alkyl-LABs. For example, α-1-C-butyl-DNJ (**19**) is 92-fold and 119-fold less active on maltase and sucrase than the corresponding α-1-C-butyl-LAB (**1c**). In contrast, α-1-C-octyl-DNJ (**21**) is 625-fold

more potent as an isomaltase inhibitor than α-1-C-octyl-LAB (**1g**). These results suggest that the change from LAB to DNJ in the iminosugar portion of the molecule results in a dramatic enhancement in enzyme specificity and α-1-C-alkyl-LAB was clearly different from α-1-C-alkyl-DNJ. For comparison, we next investigated whether the introduction of different substituents in the anomeric position had an influence on the inhibition activities of intestinal maltase, isomaltase, and sucrase (Table 5). Changing the butyl group to a 4-phenylbutyl group or a 4-methylpentyl group at the C-1 position results in a greater specificity for inhibiting maltase; **1k** and **1l** showed almost the same inhibition potency against maltase, with IC$_{50}$ values of 0.22 and 0.19 μM, respectively, but its inhibition toward isomaltase and sucrose was reduced. It is noteworthy that the C-1′ OH group dramatically changed the inhibition potency and spectrum. We previously reported that the 1-C-hydroxymethyl derivative of LAB, as in L-DMDP, was found to display inhibitory activity toward intestinal maltase, isomaltase, and sucrase, with IC$_{50}$ values of 1.2, 0.77, and 0.62 μM, respectively.[43] These values are comparable to those of LAB. In contrast, remarkable reductions in isomaltase inhibition were observed in the case of α-1-C-{(R)-1-hydroxybutyl}-LAB (**8**), which is indeed a 1004-fold weaker inhibitor than L-DMDP, while α-1-C-{(S)-1-hydroxybutyl}-LAB (**7**) showed a comparable inhibition toward maltase and sucrase. The N-butylation (**17**) and 3-C-butylation (**18**) of α-1-C-butyl-LAB obviously decreased the affinity for these α-glucosidases. Acarbose showed inhibitory activity against maltase and sucrase, with IC$_{50}$ values of 0.18 and 2.9 μM, respectively. However, acarbose exhibited less than a 50% inhibition of isomaltase even at concentrations as high as 1000 μM. Voglibose was found to be a much stronger inhibitor than acarbose. The IC$_{50}$ inhibitory activities toward maltase, isomaltase, and sucrase were 0.12, 5.2, and 37 μM, respectively. Miglitol showed potent inhibitory activity against maltase and sucrase, with IC$_{50}$ values of 1.3 and 1 μM, respectively, but these values were weaker than those of voglibose. In addition, the most striking difference between miglitol and α-1-C-butyl-LAB is that miglitol showed an unfavorable inhibition against rat intestinal cellobiase and lactase, with IC$_{50}$ values of 164 and 41 μM, respectively,

Table 3. Concentration of Iminosugars Giving 50% Inhibition of Various Glycosidases

IC$_{50}$ (μM)

Enzyme	LAB	N-Butyl-LAB	1-C-Butyl-LAB (1c)	DNJ	N-Butyl-DNJ	α-1-C-Butyl-DNJ
α-Glucosidase						
Rat intestinal maltase	0.93	63	0.13	0.36	2.1	12
Rat intestinal isomaltase	0.36	54	4.7	0.30	2.7	0.45
Rat intestinal sucrase	1.0	73	0.032	0.21	58	3.8
β-Glucosidase						
Rat intestinal cellobiase	NI[a]	NI	NI	520	NI	NI
Bovine liver	NI	NI	NI	210	NI	120
Human β-glucocerebrosidase	NI	NI	NI	195	399	70
β-Galactosidase						
Rat intestinal lactase	415	NI	NI	26	274	230
Bovine liver	NI	NI	NI	NI	NI	152
Trehalase						
Rat intestinal trehalase	75	NI	NI	42	38	167
Porcine kidney	131	NI	NI	41	36	172

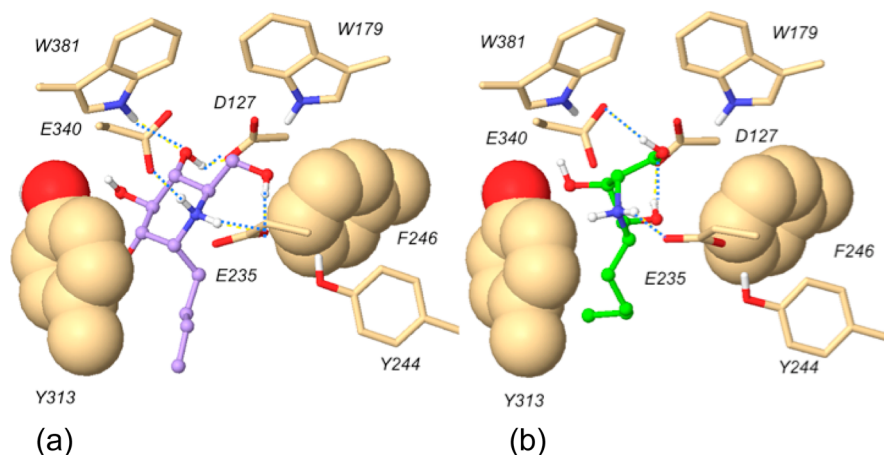[a]NI = no inhibition (less than 50% inhibition at 1000 μM).

Figure 1. Docking view of (a) α-1-C-butyl-DNJ and (b) α-1-C-butyl-LAB with human β-glucocerebrosidase.

Table 4. Inhibitory Activity (IC$_{50}$), IFDScore, and Binding Energy of α-1-C-Butyl-DNJ and α-1-C-Butyl-LAB for Human β-Glucocerebrosidase

	IC$_{50}$ (μM)	IFDScore	Δ(IFDScore)	ΔE (kcal/mol)	ΔΔE (kcal/mol)
α-1-C-butyl-DNJ	70	−890.68	−1.53	−219.08	−33.21
α-1-C-butyl-LAB	NI[a]	−889.14	0.00	−185.87	0.00

[a]NI = less than 50% inhibition at 1000 μM.

whereas α-1-C-butyl-LAB had no effect on these enzymes (data not shown). On the basis of a comparison of these commercially available inhibitors, the α-1-C-butyl-LAB prepared in this study obviously has potential for clinical use.

Structural Modification of Whole Cell N-Linked Oligosaccharides. The lumen of the endoplasmic reticulum (ER) is a highly specialized compartment for the folding and oligomeric assembly of secretory proteins, plasma membrane proteins, and proteins destined for the various organelles of the vacuolar system.[44,45] The conformational maturations of these functional glycoproteins are determined not only by the amino acid sequence but also by post-translational modifications and by a variety of chaperones and folding enzymes such as ER α-glucosidases and α-mannosidases.[46,47] The N-linked glycosylation of nascent proteins involves the transfer of Glc$_3$Man$_9$GlcNAc$_2$ from a dolichol precursor to the asparagine residue of the Asn-X-Ser/Thr glycosylation sequon of a protein. The oligosaccharide is subsequently processed by the sequential action of trimming glycosidases in the ER, prior to the production of hybrid and complex oligosaccharide structures in the Golgi.[48,49] This process of trimming commences with ER α-glucosidase I, which removes the outer α-1,2-linked glucose residue from the oligosaccharide, followed by the removal of the remaining two glucose residues through the action of an ER α-glucosidase II. In many cases, misfolded and genetic mutant
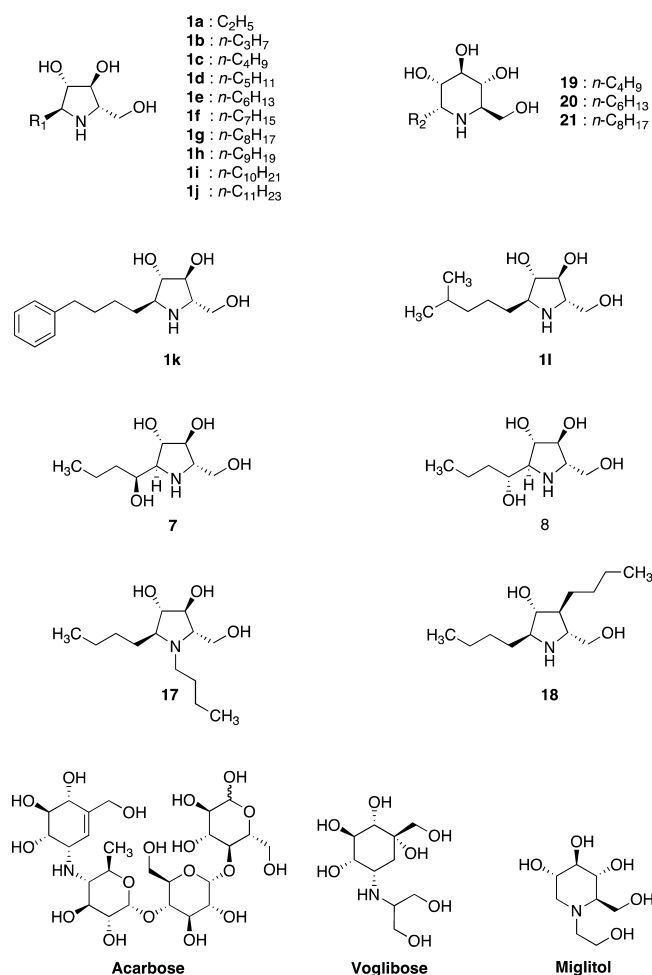
Figure 2. Chemical structures of α-1-C-alkylated LAB derivatives and sugar-mimic α-glucosidase inhibitors.

Structure labels from figure:

1a : C$_2$H$_5$
1b : n-C$_3$H$_7$
1c : n-C$_4$H$_9$
1d : n-C$_5$H$_{11}$
1e : n-C$_6$H$_{13}$
1f : n-C$_7$H$_{15}$
1g : n-C$_8$H$_{17}$
1h : n-C$_9$H$_{19}$
1i : n-C$_{10}$H$_{21}$
1j : n-C$_{11}$H$_{23}$

19 : n-C$_4$H$_9$
20 : n-C$_6$H$_{13}$
21 : n-C$_8$H$_{17}$

1k, 1l, 7, 8, 17, 18, Acarbose, Voglibose, Miglitol

Table 5. IC$_{50}$ Values (μM) for α-1-C-Alkyl-LAB against Intestinal α-Glucosidases, Compared with α-1-C-Alkyl-DNJs 19 and 20, Acarbose, Voglibose, and Miglitol

compound	IC$_{50}$ (μM)		
	maltase	isomaltase	sucrase
α-1-C-ethyl-LAB (1a)	2.6	11	0.68
α-1-C-propyl-LAB (1b)	1.7	47	0.26
α-1-C-butyl-LAB (1c)	0.13	4.7	0.032
α-1-C-pentyl-LAB (1d)	0.71	18	0.19
α-1-C-hexyl-LAB (1e)	0.51	11	0.11
α-1-C-heptyl-LAB (1f)	0.38	16	0.24
α-1-C-octyl-LAB (1g)	0.32	75	0.45
α-1-C-nonyl-LAB (1h)	0.84	171	1.4
α-1-C-decyl-LAB (1i)	1.2	606	1.7
α-1-C-undecyl-LAB (1j)	3.9	NI	13
α-1-C-(4-phenylbutyl)-LAB (1k)	0.22	14	0.31
α-1-C-(4-methylpentyl)-LAB (1l)	0.19	12	0.24
α-1-C-{(S)-1-hydroxybutyl}-LAB (7)	3.3	96	0.68
α-1-C-{(R)-1-hydroxybutyl}-LAB (8)	89	773	5.7
N-butyl-α-1-C-butyl-LAB (17)	25	NI	8.8
1,3-C-dibutyl-LAB (18)	NI^a	NI	NI
α-1-C-butyl-DNJ (19)	12	0.45	3.8
α-1-C-hexyl-DNJ (20)	4.7	0.31	2.4
α-1-C-octyl-DNJ (21)	2.1	0.12	1.5
acarbose	0.18	NI	2.9
voglibose	0.12	5.2	0.37
miglitol	1.3	39	1.0

^{a}NI = less than 50% inhibition at 1000 μM.

proteins are retained in the ER and are eventually degraded by ER-associated degradation (ERAD).[47,50,51] Thus, considering the fact that α-glucosidase inhibitors could be clinically used as antidiabetes agents, it is important that they do not disrupt the folding and maturation processes of glycoproteins. Previous studies have reported that DNJ, which is a parent compound of miglitol, inhibited not only intestinal α-glycosidases but also the processing ER enzymes α-glucosidase I and II.[52,53] Therefore, the use of DNJ could drastically change the glycan structures on glycoproteins, since it could prevent the transformation of high mannose- or hybrid-type glycans into complex-type glycans. To examine the effect of miglitol and α-1-C-butyl-LAB on whole cell N-linked oligosaccharide structures, we used the recently established chemoselective glycoblotting technique and MALDI-TOF MS analysis.[54] Human hepatocellular carcinoma HepG2 cells were treated with either 500 μM miglitol or 500 μM α-1-C-butyl-LAB for 48 h. All of the N-linked oligosaccharides were selectively captured onto new high-density hydrazide beads, which permitted them to be efficiently purified from cell homogenates. The captured N-linked oligosaccharides were subjected to on-bead methyl esterification to stabilize the sialic acids for the simultaneous quantitation of neutral and sialylated oligosaccharides by MALDI-TOF MS. As shown in Figure 3b and Table 6, a 48 h treatment with 500 μM miglitol resulted in immature Glc$_3$Man$_9$GlcNAc$_2$ (m/z 2799), Glc$_2$Man$_9$GlcNAc$_2$ (m/z

2637), and Glc$_1$Man$_9$GlcNAc$_2$ (m/z 2475) being accumulated. The presence of these glucose-residue-containing oligosaccharide structures is highly indicative of the inhibition of the processing enzymes α-glucosidase I and II. In sharp contrast, the control and α-1-C-butyl-LAB had very similar patterns (Figure 3a,c). These results clearly indicate that there is a risk associated with the use of miglitol, since it could increase the expression of immature high-mannose-type N-linked oligosaccharides, whereas α-1-C-butyl-LAB did not appear to have any effect on the processing α-glucosidases.

Carbohydrate Loading Test. A recent metaregression analysis revealed that 2 h postprandial glucose levels and cardiovascular risk were closely related.[10] Furthermore, there is a substantial body of epidemiological evidence that points to an association between postprandial hyperglycemia and macrovascular complications.[12,55] Therefore, α-glucosidase inhibitors have considerable potential for reducing the risk of these diseases. The iminosugar-based α-glucosidase inhibitor miglitol differs from carbasugar-type α-glucosidase inhibitors such as acarbose and voglibose, because it is rapidly and completely absorbs in the upper region of the small intestine.[31] This pharmacokinetic property consequently enables the strong and early phase suppression of postprandial hyperglycemia, with no or minimal gastrointestinal complications. We then investigated the influence of α-1-C-butyl-LAB and miglitol, which was used as a positive control, on blood glucose levels after an in vivo maltose loading (Figure 4). The control group was loaded with saline only. When compared to the control, α-1-C-butyl-LAB caused significantly lower blood glucose levels at 15 and 30 min compared to a placebo administration (Figure 4b). Moreover, treatment with α-1-C-butyl-LAB led to a 43.9% decrease of the area under the curve (AUC) at a dose of 0.25 mg/kg of body weight. It was interesting to note that the remaining blood
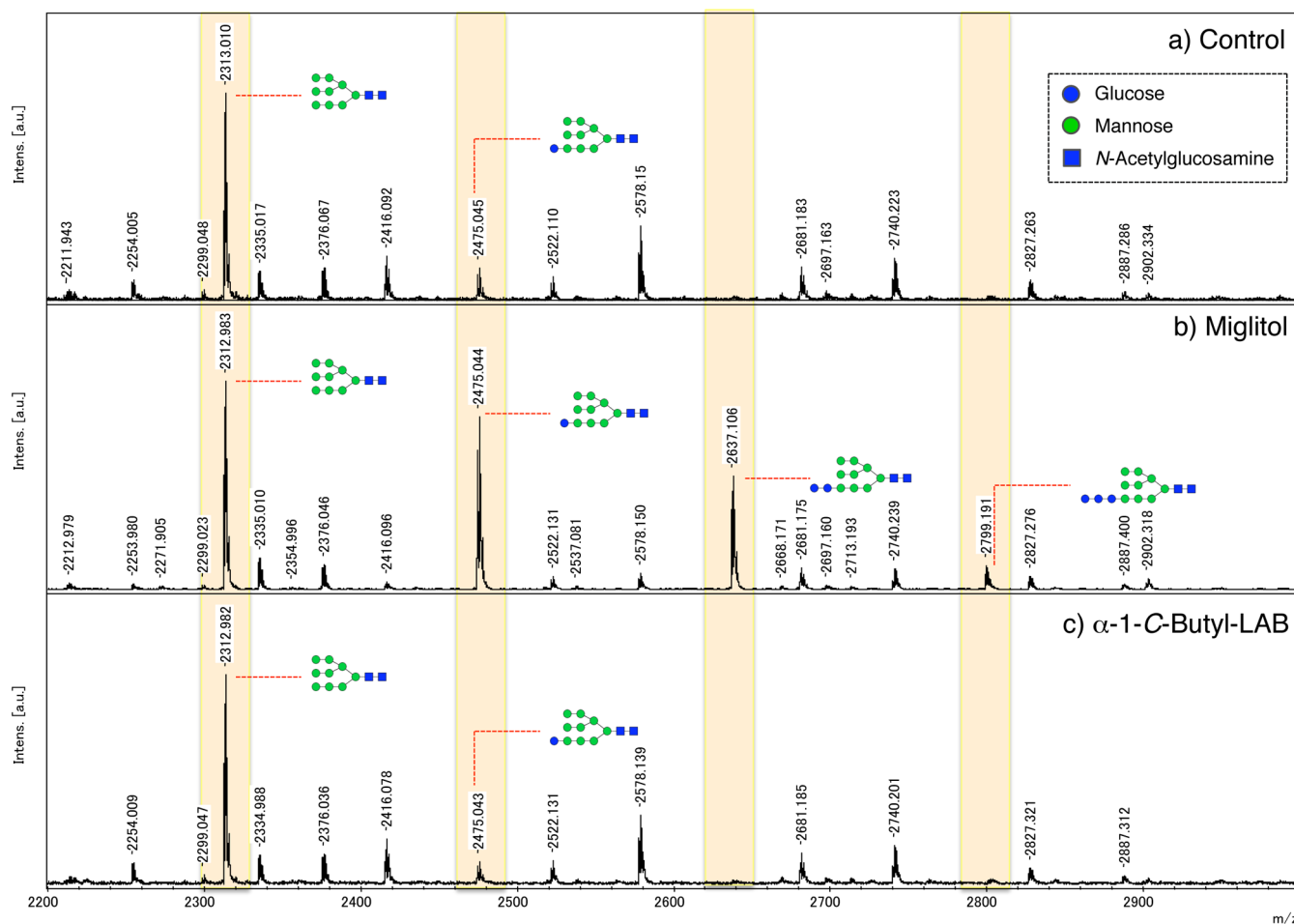
Figure 3. MALDI-TOF MS spectra showing the effects of α-glucosidase-inhibiting iminosugars on whole cell glycoproteins. Relative expression levels of glucose residues containing *N*-linked oligosaccharides on human hepatocelluar carcinoma HepG2 cells cultured for 48 h with or without 500 μM (b) miglitol and (c) α-1-*C*-butyl-LAB. Structural identification of glycans was performed by MS analysis and the use of a database for glycan structures (http://web.expasy.org/glycomod/).

Table 6. Structures and Proportion (%) of Isolated Whole Cell *N*-Linked Oligosaccharide Peaks from the Control and 500 μM Miglitol- and 500 μM α-1-*C*-Butyl-LAB-Treated HepG2 Cells

● Glucose ● Mannose ■ *N*-Acetylglucosamine					
m/z	Estimated glycan composition ('GlycoMod' database)	Structure:	% Area		
			Control	α-1-*C*-butyl-LAB	Miglitol
2313	$(Hex)_6 + (Man)_3(GlcNAc)_2$		5.96	7.13	10.67
2475	$(Hex)_7 + (Man)_3(GlcNAc)_2$		1.22	1.02	9.63
2637	$(Hex)_8 + (Man)_3(GlcNAc)_2$		0.00	0.00	6.69
2799	$(Hex)_9 + (Man)_3(GlcNAc)_2$		0.00	0.00	1.54

glucose levels were slightly higher with α-1-*C*-butyl-LAB than with the placebo at 60 and 120 min (Figure 4b). This behavior with strong and early phase suppression of postprandial hyperglycemia was similar to that observed for miglitol (Figure 4a). For comparison, we next investigated the influence of α-1-*C*-butyl-LAB using a sucrose loading test (Figure 5). The administration of sucrose (2.5 g/kg of body weight, po) to fasted mice resulted in a rapid increase in blood glucose concentrations from 80 ± 8 mg/dL to a maximum of 181 ± 16

mg/dL after 30 min. Thereafter blood glucose levels recovered to the pretreatment level at 120 min. α-1-*C*-Butyl-LAB resulted in significantly lower blood glucose levels at 15, 30, and 60 min than placebo administration (Figure 5b). Moreover, the AUC for plasma glucose from 0 to 60 min after α-1-*C*-butyl-LAB administration was reduced by 49.1% at a dose of 0.1 mg/kg of body weight and 69.2% at a dose of 0.5 mg/kg of body weight, compared with the AUC for the control. This behavior was similar to that observed for miglitol administration (Figure 5a).
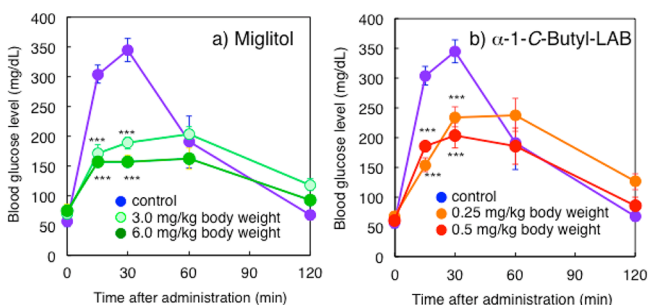
Figure 4. Effects of miglitol (a) and α-1-C-butyl-LAB (b) on blood glucose levels. Blood glucose concentrations of male ddY mouse after an oral load with maltose, 2.5 g/kg of body weight, with (a) 3.0 (light green) and 6.0 (green) mg/kg of body weight miglitol and (b) 0.25 (orange) and 0.5 (red) mg/kg of body weight α-1-C-butyl-LAB. The control group was loaded with saline (purple). Each value represents the mean $\pm$ SEM (n = 5). Three asterisks indicate a significant difference ($p < 0.001$) compared with the control.
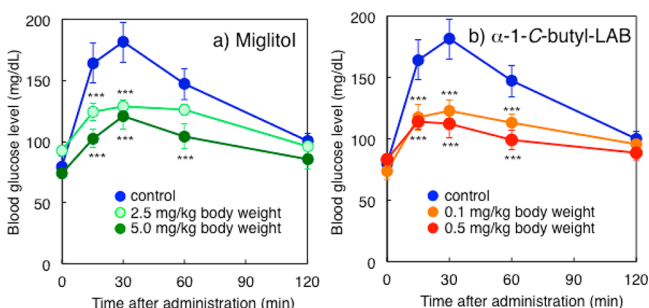

Figure 5. Effects of miglitol (a) and α-1-C-butyl-LAB (b) on blood glucose levels. Blood glucose concentrations of male ddY mouse after an oral load with sucrose, 2.5 g/kg of body weight, with (a) 2.5 (light green) and 5.0 (green) mg/kg of body weight miglitol and (b) 0.1 (orange) and 0.5 (red) mg/kg of body weight α-1-C-butyl-LAB. The control group was loaded with saline (blue). Each value represents the mean $\pm$ SEM (n = 5). Three asterisks indicate a significant difference ($p < 0.001$) compared with the control.

The administration of miglitol led to the suppression of the blood glucose levels in a dose-dependent manner; as a consequence, the AUC for plasma glucose from 0 to 60 min after miglitol administration was reduced by 40.5% at a dose of 2.5 mg/kg of body weight and 58.7% at a dose of 5.0 mg/kg of body weight. Remarkably, the effective doses of α-1-C-butyl-LAB were about 10 times lower than those of miglitol in both disaccharide loading tests. The LAB derivative showed a suppressive effect against postprandial hyperglycemia at a does of only 0.1−0.5 mg/kg of body weight (Figures 4 and 5). A recent study suggested that miglitol suppresses glucose levels via two different mechanisms, namely, the direct inhibition of α-glucosidase and, indirectly, via affecting the secretion of GLP-1.[56,57] GLP-1 is released from the intestine in response to nutrients and exerts a potent insulin-releasing effect on pancreatic β-cells.[32,33] The important point to note is that the GLP-1 release effect appears only when it is administered orally.[13] Further studies will clearly be needed to more completely understand the mechanisms of α-1-C-butyl-LAB, but our results could be interpreted to mean that it affects to GLP-1 secretion because this compound is not only an iminosugar but also an absorbable α-glucosidase inhibitor similar to miglitol. On the basis of these findings and by comparison with our results for miglitol, it appears that α-1-C-

butyl-LAB is absorbed from the upper region of the small intestine, much the same as miglitol, and it causes less diarrhea than acarbose and voglibose.

Docking Studies of α-1-C-Butyl-LAB and Miglitol with Intestinal Maltase. In piperidine pyranoside mimics such as α-1-C-butyl-DNJ and miglitol, there is usually a good overlap between the structure of the glycoside and inhibition by the corresponding iminosugar mimic. However, α-1-C-butyl-LAB is an unusual L-type pyrrolidine iminosugar, and it does not seem to overlap extensively with D-type piperidine iminosugars. To understand the structural basis of the interaction of α-1-C-butyl-LAB and miglitol with maltase, we first determined the mode of inhibition and the inhibition constant (K_i) of miglitol and α-1-C-butyl-LAB from Lineweaver−Burk plots. As shown in Figure 6, miglitol and α-1-C-butyl-LAB inhibited maltase in a
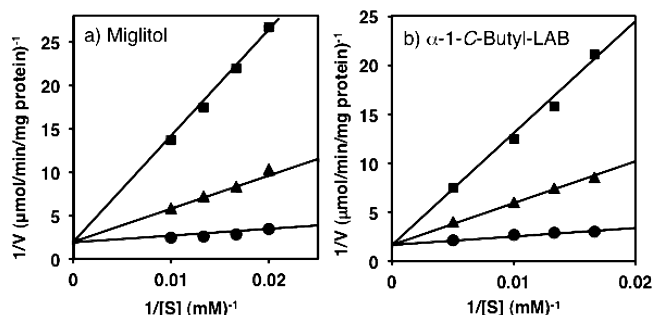

Figure 6. Lineweaver−Burk plots of miglitol (a) and α-1-C-butyl-LAB (b) inhibition of rat intestinal maltase. An increasing concentration of maltose or sucrose was used to determine the K_i values, and the data were plotted as $1/V$ versus $1/[S]$. (a) The concentrations of miglitol were 0 μM (closed circles), 2.0 μM (closed triangles), and 5.0 μM (closed squares). The calculated K_i value was 0.46 μM. (b) The concentrations of α-1-C-butyl-LAB were 0 μM (closed circles), 0.2 μM (closed triangles), and 0.75 μM (closed squares). The calculated K_i value was 0.085 μM.

competitive manner, with K_i values of 0.46 and 0.085 μM, respectively. This result suggests that α-1-C-butyl-LAB occupies the active site of this enzyme, much the same as miglitol. Thus, we next attempted to construct three-dimensional structures of the N-terminal catalytic domain of maltase-glucoamylase (ntMGAM) of rat complexed with α-1-C-butyl-LAB. For comparison, we also constructed three-dimensional structures of rat ntMGAM complexed with α-1-C-butyl-DNJ or miglitol. As shown in Figure 7, α-1-C-butyl-LAB, α-1-C-butyl-DNJ, and miglitol were observed to bind to the hydrophobic pocket consisting of Trp376, Trp516, Trp613, and Phe649 of rat ntMGAM. However, it was suggested that the orientations of the butyl groups of α-1-C-butyl-LAB and α-1-C-butyl-DNJ are different. The butyl group of α-1-C-butyl-LAB has a favorable interaction with the hydrophobic pocket (Trp376, Leu405, and Ile441), while the butyl groups of α-1-C-butyl-DNJ bind to the other hydrophobic pocket (Trp481, Met519) (Figure 7). The interaction between the butyl group of α-1-C-butyl-LAB and the hydrophobic pocket of ntMGAM looks important for ligand binding, which conforms to the study[58] by Aguilar-Moncayo et al. pointing out the critical role of aglyconic interactions in glycosidase binding. The hydroxyethyl group of miglitol also binds to the same hydrophobic pocket as α-1-C-butyl-DNJ, but miglitol has an additional interaction with hydrophilic residues (Asp616 and Arg600) of rat ntMGAM. The interactions between rat ntMGAM and α-1-C-butyl-LAB,
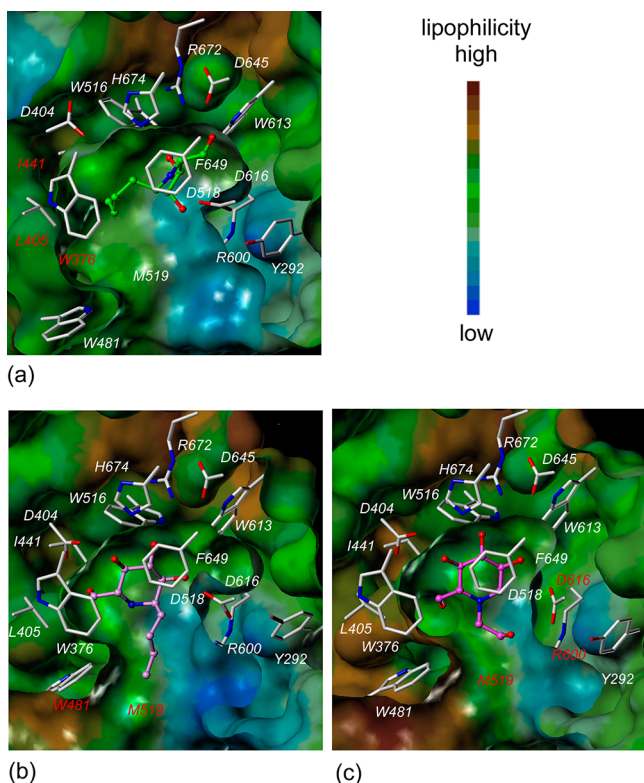
(a)

(b)

(c)

Figure 7. View of interactions of (a) α-1-C-butyl-LAB, (b) α-1-C-butyl-DNJ, and (c) miglitol with rat ntMGAM.

(a)

(b)

(c)

Figure 8. Schematic interaction diagrams between rat ntMGAM and (a) α-1-C-butyl-LAB, (b) α-1-C-butyl-DNJ, and (c) miglitol. Hydrogen bonds are depicted by dashed lines.

α-1-C-butyl-DNJ, or miglitol are illustrated in Figure 8. Miglitol and α-1-C-butyl-DNJ are positioned to form hydrogen bonds with Asp404, Asp518, Asp616, and His674 of rat ntMGAM, while α-1-C-butyl-LAB can form hydrogen bonds with Asp518, Asp616, Trp613, and Asp645 of rat ntMGAM. For the purpose of clarifying the difference, the binding energies between the compounds and rat ntMGAM were calculated. The binding energies (ΔE) for α-1-C-butyl-LAB, α-1-C-butyl-DNJ, and miglitol were −269.97, −236.53, and −261.36 kcal mol^{-1} (Table 7). These results were consistent with the experimental results (IC$_{50}$) showing that miglitol and α-1-C-butyl-LAB have higher inhibitory activities against maltase of rat ntMGAM than α-1-C-butyl-DNJ. For further confirmation, we also constructed the three-dimensional models of the α-1-C-butyl-LAB−human ntMGAM complex. The docking calculation was performed under the same conditions as the docking calculations of rat ntMGAM using the X-ray structures of human ntMGAM (PDB IDs 2QLY, 2QMJ, 3CTT, and 3L4W). The binding energy (ΔE), as estimated from the three-dimensional structures of the compound with human ntMGAM, suggested that α-1-C-butyl-LAB would be an inhibitor of human maltase as well as that from the rat (Table 8). Furthermore, the binding free energy (ΔG) estimated by the MM-GBSA method using Prime in the Schrödinger Suite strongly supported that α-1-C-butyl-LAB has inhibition activity in human ntMGAM.

■ CONCLUSIONS

In this study, we report on the design and synthesis of a series of α-1-C-alkylated LAB derivatives by AAA, RCM, and Negishi cross-coupling as key reactions. Among the produced compounds, α-1-C-butyl-LAB showed potent inhibitory activity toward intestinal maltase, isomaltase, and sucrase, with IC$_{50}$ values of 0.20, 4.7, and 0.032 μM, respectively. The following
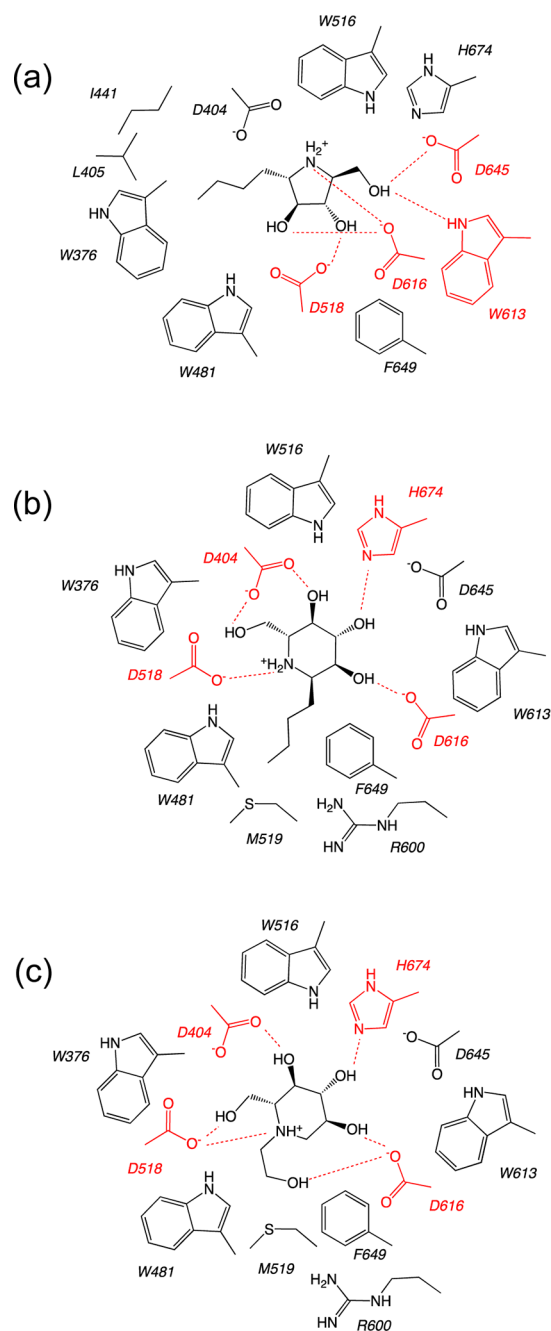
Table 7. Inhibitory Activity (IC$_{50}$) and Binding Energy (ΔE) of α-1-Butyl-LAB, α-1-Butyl-DNJ, and Miglitol with Rat ntMGAM

	IC$_{50}$ (μM)	ΔE (kcal/mol)
α-1-C-butyl-LAB	0.13	−269.97
α-1-C-butyl-DNJ	12	−236.53
miglitol	1.3	−261.36

are the main features of α-1-C-butyl-LAB: (a) It does not inhibit intestinal β-glycosidases and lysosomal β-glucocerebrosidase even at concentrations as high as 1000 μM. (b) MALDI-TOF MS analysis revealed that it obviously differs from miglitol in that it does not disrupt oligosaccharide processing and the

Table 8. Binding Energy (ΔE) and Binding Free Energy (ΔG) Estimated for α-1-C-Butyl-LAB with Human and Rat ntMGAM

	ΔE (kcal/mol)	ΔG (kcal/mol)
rat ntMGAM	−269.97	−42.13
human ntMGAM	−260.51	−46.99

maturation of glycoproteins. (c) It showed a strong and early phase suppression of postprandial hyperglycemia, and the effective dose was 10 times lower than that for miglitol. (d) Both α-1-C-butyl-LAB and miglitol are competitive inhibitors, whereas molecular docking studies revealed that the interaction modes and the orientations of the alkyl chain of α-1-C-butyl-LAB and miglitol are clearly different. Each alkyl group has a favorable interaction, but with different hydrophobic pockets. (e) Docking calculations using X-ray structures of human ntMGAM (PDB IDs 2QLY, 2QMJ, 3CTT, and 3L4W) suggested that the binding conformations and orientations of α-1-C-butyl-LAB and miglitol in human ntMGAM are similar to those in rat ntMGAM. α-1-C-Butyl-LAB therefore represents a new class of promising compounds that have the potential for treating postprandial hyperglycemia.

■ EXPERIMENTAL SECTION

General Experimental Procedures. Infrared (IR) spectra were recorded on a Perkin-Elmer 1600 series FT-IR spectrometer. Mass spectra were recorded on a JEOL JMN-DX 303/JMA-DA 5000 spectrometer. Microanalyses were performed on a Perkin-Elmer CHN 2400 elemental analyzer. Optical rotations were measured with a JASCO DIP-360 or JASCO P-1020 digital polarimeter. Proton nuclear magnetic resonance (^{1}H NMR) spectra were recorded on a JEOL JNM-EX 270 (270 MHz), Varian Gemini-300 (300 MHz), JEOL JNM-AL 400 (400 MHz), Varian Unity-500 (500 MHz), or JNM-LA (600 MHz) spectrometer using tetramethylsilane as the internal standard. The following abbreviations are used: s = singlet, d = doublet, t = triplet, q = quartet, m = multiplet, br = broad. Column chromatography was carried out on Merck silica gel 60 (230−400 mesh) or KANTO silica gel 60N (40−50 mm) for flash chromatography. The purity of all final compounds was established to be ≥95% by HPLC analysis (Agilent 1220 Infinity LC system). HPLC conditions: TSKgel NH$_2$-100 3 μm column (4.6 mm ×15 cm) using CH$_3$CN/H$_2$O = 90/10 (flow rate 1.0 mL/min) as the eluent and refractive index detector (retention time 17.2 min for compound **1c**).

Preparation of Iminosugars and Their Alkyl Derivatives. 1-Deoxynojirimycin was isolated from the roots of *Adenophora triphylla* according to the literature.[59] The 1-C-alkyl-DNJ derivatives **19−21** were prepared according to the method reported previously.[60,61] LAB was prepared from xylitol according to the literature.[62] The N-butylation of LAB and DNJ was performed by treatment with the butyl bromide and K$_2$CO$_3$ in dimethylformamide. The reaction mixture was evaporated in vacuo, and the residual syrup was redissolved in MeOH and applied to an Amberlist 15 column (H$^+$ form), eluted with 0.5 M NH$_4$OH, and concentrated. The eluate was finally purified by Dowex 1-X2 (OH$^-$ form) and Amberlite CG-50 (NH$_4^+$ form) column chromatography with water as the eluent. Acarbose was purchased from LKT Laboratories Inc. (St. Paul, MN). Voglibose and miglitol were purchased from Wako Pure Chemical Industries, Ltd. (Osaka, Japan).

Typical Procedure for α-1-C-Alkyl-LAB. *Preparation of (5R,7aR)-5-(Iodomethyl)-1,7a-dihydropyrrolo[1,2-c]oxazol-3(5H)-one (2).* Iodine chips (11.3 g, 44.5 mmol) were added to a solution of alcohol **3** (3.45 g, 22.2 mmol), triphenylphosphine (14.6 g, 55.6 mmol), and imidazole (3.79 g, 55.6 mmol) in CH$_2$Cl$_2$ (89 mL) at 0 °C. After being stirred at room temperature for 6 h, the reaction was quenched with 1.0 M aq sodium thiosulfate. The water layer was extracted with CH$_2$Cl$_2$ (2 × 40 mL). The organic layers were

combined and dried over anhydrous Na$_2$SO$_4$. Filtration and evaporation in vacuo furnished the crude product, which was purified by column chromatography (silica gel, 80 g, hexane/EtOAc = 2/1) to provide **2** (5.16 g, 88%) as a pale yellow oil. $[\alpha]_D^{23}$ = +141.6 (CHCl$_3$, c = 1.00). ^{1}H NMR (CDCl$_3$, 400 MHz): δ 3.29−3.37 (m, 2H), 4.24 (dd, J = 8.7, 6.8 Hz, 1H), 4.64 (t, J = 8.7 Hz, 1H), 4.79 (br s, 1H), 4.86−4.90 (m, 1H), 6.03 (d, J = 6.3 Hz, 1H), 6.08 (d, J = 6.8 Hz, 1H). ^{13}C NMR (CHCl$_3$, 100 MHz): δ 8.60, 64.51, 67.20, 68.84, 130.73, 133.28, 162.11. IR (neat, cm^{-1}): 1749. HRMS (EI): m/z calcd for C$_7$H$_8$NO$_2$I (M$^+$) 264.9600, found 264.9603.

Preparation of Alkylzinc Bromide (n-Propylzinc Bromide). Iodine chips (127 mg, 0.50 mmol) were added to a suspension of zinc powder (981 mg, 15.0 mmol) in N,N-dimethylacetamide (10 mL) at room temperature. After being stirred for 10 min, the resulting mixture changed from a dark brown suspension to a colorless suspension. 1-Bromopropane (0.91 mL, 10.0 mmol) was added by syringe, and the reaction mixture was stirred at 80 °C for 3 h. The concentration in N,N-dimethylacetamide was ~0.75 M.

Typical Procedure for Negishi Coupling (4c). Yellow bis(1,5-cyclooctadiene)nickel(0) (48.4 mg, 0.176 mmol, 16 mol %) and (S,S)-2,6-bis(4-isopropyl-2-oxazolin-2-yl)pyridine (106 mg, 0.352 mmol, 32 mol %) were added to N,N-dimethylacetamide (7.0 mL) under an argon atmosphere, and the resulting mixture was stirred for 30 min at room temperature. The resulting deep-blue solution was added to a solution of the n-propylzinc bromide (in N,N-dimethylacetamide, 4.7 mL, 3.52 mmol) and **2** (291 mg, 1.10 mmol). After being stirred for 20 h, the reaction was quenched with iodine chips (440 mg). After being stirred for 10 min, the dark-brown mixture was passed through a short pad of silica gel (eluting with AcOEt/hexane = 1/1) (to remove N,N-dimethylacetamide, inorganic salts, and iodine). The filtrate was then concentrated, and the residue was purified by flash chromatography (silica gel, 20 g, eluting with hexane/EtOAc = 3/1) to provide **4c** (156 mg, 78%) as a colorless oil.

(5S,7aR)-5-Butyl-1,7a-dihydropyrrolo[1,2-c]oxazol-3(5H)-one (4c). $[\alpha]_D^{24}$ = +175.4 (CHCl$_3$, c = 1.08). ^{1}H NMR (CDCl$_3$, 400 MHz): δ 0.91 (t, J = 6.8 Hz, 3H), 1.34−1.58 (m, 6H), 4.20 (dd, J = 8.2, 5.3 Hz, 1H), 4.54 (br s, 1H), 4.58 (t, J = 8.7 Hz, 1H), 4.72−4.77 (m, 1H), 5.85 (ddd, J = 6.3, 1.4 Hz, 1H), 6.02 (ddd, J = 6.3, 2.4 Hz, 1H). ^{13}C NMR (CHCl$_3$, 100 MHz): δ 13.94, 22.44, 28.30, 34.02, 63.82, 67.41, 68.72, 127.97, 135.23, 162.98. IR (neat, cm^{-1}): 2930, 1752. HRMS (EI): m/z calcd for C$_{10}$H$_{15}$NO$_2$ (M$^+$) 181.1103, found 181.1099.

Typical Procedure for Epoxidation (5c). To a vial with **4c** (158.0 mg, 0.872 mmol) were added 6.4 mL of CH$_3$CN and 4.4 mL of 4 × 10^{-4} M ethylenediaminetetraacetic acid in H$_2$O. The solution was cooled to 0 °C, and 1,1,1-trifluoroacetone (977 mg, 8.72 mmol) was added. A mixture of solid Oxone (2.68 g, 4.36 mmol) and NaHCO$_3$ (549 mg, 6.54 mmol) was added in four portions over 45 min. The reaction was stirred for 2 h at 0 °C, then diluted with 5 mL of H$_2$O, and extracted with CH$_2$Cl$_2$ (3 × 15 mL). The organic layers were combined and dried over anhydrous Na$_2$SO$_4$. Filtration and evaporation in vacuo furnished the crude product (231 mg), which was purified by column chromatography (silica gel, 6 g, Et$_2$O) to provide epoxide **5c** (171 mg, 99%) as a colorless oil.

(1aR,1bS,6S,6aS)-6-Butyltetrahydrooxireno[2′,3′:3,4]pyrrolo[1,2-c]oxazol-4(1aH)-one (5c). $[\alpha]_D^{22}$ = +48.2 (CHCl$_3$, c = 0.12). ^{1}H NMR (CDCl$_3$, 400 MHz): δ 0.90 (t, J = 7.2 Hz, 3H), 1.26−1.58 (m, 6H), 3.54 (d, J = 2.9 Hz, 1H), 3.61 (d, J = 2.9 Hz, 1H), 3.97 (dd, J = 8.7, 4.3 Hz, 1H), 4.03 (dd, J = 9.2, 4.8 Hz, 1H), 4.46 (dd, J = 9.2, 4.3 Hz, 1H), 4.53 (t, J = 8.7 Hz, 1H). ^{13}C NMR (CDCl$_3$, 100 MHz): δ 13.91, 22.39, 28.19, 29.73, 55.27, 57.20, 58.77, 60.42, 64.65, 162.56. IR (neat, cm^{-1}): 2959, 2933, 1754. HRMS (EI): m/z calcd for C$_{10}$H$_{15}$NO$_3$ (M$^+$) 197.1052, found 197.1054.

Typical Procedure for the Preparation of a Diol (6c). Trifluoroacetic acid (0.78 mL, 10.5 mmol) was added to a solution of the epoxide **5c** (171 mg, 0.867 mmol) in THF/H$_2$O (3/2, 7.5 mL). After being stirred at 80 °C for 72 h, the reaction mixture was cooled to room temperature and concentrated. The product was purified by flash chromatography (silica gel, 10 g, Et$_2$O only → Et$_2$O/CH$_3$OH = 20/1) to yield diol **6c** (136 mg, 74%) as a colorless oil.

(5S,6S,7S,7aS)-5-Butyl-6,7-dihydroxytetrahydropyrrolo[1,2-c]-oxazol-3(1H)-one (6c). $[\alpha]_D^{23}$ = +22.2 (CHCl$_3$, c = 0.46). ^{1}H NMR (CDCl$_3$, 400 MHz): δ 0.90−0.95 (m, 3H), 1.25−1.69 (m, 6H), 3.65−3.67 (m, 1H), 3.84−3.88 (m, 1H), 3.90−3.98 (m, 2H), 4.34 (dd, J = 9.7, 3.9 Hz, 1H), 4.52 (dd, J = 9.2, 7.7 Hz, 1H). ^{13}C NMR (CHCl$_3$, 100 MHz): δ 13.99, 22.42, 28.20, 32.81, 61.99, 65.29, 66.85, 80.93, 83.74, 162.45. IR (neat, cm^{-1}): 3377, 1731. HRMS (EI): m/z calcd for C$_{10}$H$_{17}$NO$_4$ (M$^+$) 215.1158, found 215.1162.

Typical Procedure for Hydrolysis (1c). NaOH (143 mg, 3.58 mmol) was added to a solution of diol **6c** (71.0 mg, 0.330 mmol) in EtOH/H$_2$O (2:1, 4.2 mL), and the mixture was refluxed for 12 h. The reaction mixture was cooled to room temperature and concentrated. The product was purified by flash chromatography (silica gel, 10 g, Et$_2$O/MeOH/25% NH$_3$(aq) = 80/20/1 → Et$_2$O/MeOH/25% NH$_3$(aq) = 0/100/2) to yield **1c** (38.0 mg, 61%) as a white amorphous solid.

α-1-C-Ethyl-LAB (1a). $[\alpha]_D^{24}$ = −57.9 (CH$_3$OH, c = 1.37). ^{1}H NMR (CD$_3$OD, 400 MHz): δ 0.98 (t, J = 7.5 Hz, 3H), 1.39−1.50 (m, 1H), 1.65−1.75 (m, 1H), 2.78 (dt, J = 7.7, 5.3 Hz, 1H), 2.95 (dt, J = 6.3, 4.3 Hz, 1H), 3.56−3.61 (m, 2H), 3.64−3.68 (m, 1H), 3.75 (t, J = 6.8 Hz, 1H). ^{13}C NMR (CD$_3$OD, 100 MHz): δ 11.32, 27.97, 63.29, 64.19, 64.35, 79.67, 83.34. IR (KBr, cm^{-1}): 3297, 2922. HRMS (EI): m/z calcd for C$_7$H$_{15}$NO$_3$ (M$^+$) 161.1052, found 161.1056.

α-1-C-Propyl-LAB (1b). $[\alpha]_D^{24}$ = −46.7 (CH$_3$OH, c = 1.18). ^{1}H NMR (CD$_3$OD, 400 MHz): δ 0.96 (t, J = 7.2 Hz, 3H), 1.35−1.55 (m, 3H), 1.63−1.74 (m, 1H), 2.92−2.97 (m, 1H), 3.04 (dd, J = 6.3, 3.9 Hz, 1H), 3.60−3.65 (m, 2H), 3.68−3.72 (m, 1H), 3.79 (t, J = 6.3 Hz, 1H). ^{13}C NMR (CD$_3$OD, 100 MHz): δ 14.42, 20.77, 36.83, 62.54, 62.65, 64.55, 79.00, 82.97. IR (KBr, cm^{-1}): 3223, 2929. HRMS (EI): m/z calcd for C$_8$H$_{17}$NO$_3$ (M$^+$) 175.1208, found 175.1207.

α-1-C-Butyl-LAB (1c). $[\alpha]_D^{27}$ = −47.7 (CH$_3$OH, c = 1.00). ^{1}H NMR (CD$_3$OD, 400 MHz): δ 0.93 (t, J = 6.8 Hz, 3H), 1.28−1.45 (m, 5H), 1.64−1.72 (m, 1H), 2.83 (dt, J = 7.7, 5.3 Hz, 1H), 2.94 (dt, J = 6.3, 4.3 Hz, 2H), 3.63−3.67 (m, 1H), 3.74 (t, J = 6.3 Hz, 1H). ^{13}C NMR (CD$_3$OD, 100 MHz): δ 14.33, 23.77, 29.83, 34.45, 62.67, 62.87, 64.56, 79.13, 83.10. IR (KBr, cm^{-1}): 3285. HRMS (EI): m/z calcd for C$_9$H$_{19}$NO$_3$ (M$^+$) 189.1365, found 189.1360.

α-1-C-Pentyl-LAB (1d). $[\alpha]_D^{24}$ = −53.5 (CH$_3$OH, c = 1.44). ^{1}H NMR (CD$_3$OD, 400 MHz): δ 0.91 (t, J = 7.0 Hz, 3H), 1.24−1.50 (m, 7H), 1.60−1.73 (m, 1H), 2.81−2.86 (m, 1H), 2.93−2.97 (m, 1H), 3.55−3.59 (m, 2H), 3.63−3.67 (m, 1H), 3.74 (t, J = 6.5 Hz, 1H). ^{13}C NMR (CD$_3$OD, 100 MHz): δ 14.39, 23.66, 27.46, 33.14, 35.32, 62.65, 63.34, 64.40, 79.64, 83.68. IR (KBr, cm^{-1}): 3285, 2926. HRMS (EI): m/z calcd for C$_{10}$H$_{21}$NO$_3$ (M$^+$) 203.1521, found 203.1519.

α-1-C-Hexyl-LAB (1e). $[\alpha]_D^{24}$ = −51.1 (CH$_3$OH, c = 1.18). ^{1}H NMR (CD$_3$OD, 400 MHz): δ 0.90 (t, J = 6.3 Hz, 3H), 1.25−1.48 (m, 9H), 1.62−1.72 (m, 1H), 2.86 (dd, J = 12.5, 7.2 Hz, 1H), 2.97 (dd, J = 10.9, 6.0 Hz, 1H), 3.56−3.60 (m, 2H), 3.64−3.68 (m, 1H), 3.75 (t, J = 6.5 Hz, 1H). ^{13}C NMR (CD$_3$OD, 100 MHz): δ 14.41, 23.67, 27.70, 30.54, 32.94, 35.26, 62.69, 63.23, 64.41, 79.57, 83.58. IR (KBr, cm^{-1}): 3286, 2924, 2853. HRMS (EI): m/z calcd for C$_{11}$H$_{23}$NO$_3$ (M$^+$) 217.1678, found 217.1685.

α-1-C-Heptyl-LAB (1f). $[\alpha]_D^{24}$ = −46.1 (CH$_3$OH, c = 1.00). ^{1}H NMR (CD$_3$OD, 400 MHz): δ 0.90 (t, J = 6.8 Hz, 3H), 1.20−1.50 (m, 11H), 1.60−1.75 (m, 1H), 2.84 (dd, J = 12.6, 7.7 Hz, 1H), 2.96 (dd, J = 10.6, 6.3 Hz, 1H), 3.55−3.59 (m, 2H), 3.64−3.68 (m, 1H), 3.74 (t, J = 6.5 Hz, 1H). ^{13}C NMR (CD$_3$OD, 100 MHz): δ 14.43, 23.73, 27.77, 30.39, 30.86, 33.01, 35.32, 62.67, 63.29, 64.41, 79.61, 83.64. IR (KBr, cm^{-1}): 3286, 2923. HRMS (EI): m/z calcd for C$_{12}$H$_{25}$NO$_3$ (M$^+$) 231.1834, found 231.1824.

α-1-C-Octyl-LAB (1g). $[\alpha]_D^{23}$ = −44.2 (CH$_3$OH, c = 0.70). ^{1}H NMR (CD$_3$OD, 400 MHz): δ 0.89 (t, J = 7.0 Hz, 3H), 1.30−1.47 (m, 13H), 1.67−1.73 (m, 1H), 2.89−2.94 (m, 1H), 3.01−3.06 (m, 1H), 3.59−3.63 (m, 2H), 3.69 (m, 1H), 3.77 (t, J = 6.8 Hz, 1H). ^{13}C NMR (CD$_3$OD, 100 MHz): δ 14.43, 23.73, 27.68, 30.41, 30.64, 30.82, 33.05, 34.79, 62.69, 62.98, 64.65, 79.15, 83.12. IR (KBr, cm^{-1}): 3287, 2924, 2852. HRMS (EI): m/z calcd for C$_{13}$H$_{27}$NO$_3$ (M$^+$) 245.1991, found 245.1982.

α-1-C-nonyl-LAB (1h). $[\alpha]_D^{23}$ = −45.5 (CH$_3$OH, c = 1.33). ^{1}H NMR (CD$_3$OD, 400 MHz): δ 0.89 (t, J = 6.8 Hz, 3H), 1.22−1.50 (m, 15H),

1.62−1.72 (m, 1H), 2.84 (dd, J = 12.5, 7.2 Hz, 1H), 2.97 (m, 1H), 3.55−3.60 (m, 2H), 3.64−3.68 (m, 1H), 3.74 (t. J = 6.8 Hz, 1H). ^{13}C NMR (CD$_3$OD, 100 MHz): δ 14.45, 23.73, 27.77, 30.47, 30.71, 30.89, 33.07, 35.31, 62.69, 63.28, 64.42, 79.61, 83.63. IR (neat, cm^{-1}): 3289, 2923, 2852. HRMS (EI): m/z calcd for C$_{14}$H$_{29}$NO$_3$ (M$^+$) 259.2147, found 259.2151.

α-1-C-Decyl-LAB (1i). $[\alpha]_D^{22}$ = −36.5 (CH$_3$OH, c = 0.41). ^{1}H NMR (CD$_3$OD, 400 MHz): δ 0.90 (t, J = 6.5 Hz, 3H), 1.24−1.51 (m, 17H), 1.65−1.75 (m, 1H), 2.86 (dd, J = 12.3, 7.5 Hz, 1H), 2.97 (dd, J = 10.6, 6.3 Hz, 1H), 3.57−3.61 (m, 2H), 3.67 (dd, J = 11.6, 4.3 Hz, 1H), 3.77 (t, J = 6.7 Hz, 1H). ^{13}C NMR (CD$_3$OD, 100 MHz): δ 14.45, 23.73, 27.68, 30.47, 30.67, 30.74, 30.82, 33.07, 34.81, 62.71, 62.94, 64.60, 79.18, 83.15. IR (KBr, cm^{-1}): 3289, 2923, 2852. HRMS (EI): m/z calcd for C$_{15}$H$_{31}$NO$_3$ (M$^+$) 273.2304, found 273.2304.

α-1-C-Undecyl-LAB (1j). $[\alpha]_D^{23}$ = −37.8 (CH$_3$OH, c = 1.00). ^{1}H NMR (CD$_3$OD, 400 MHz): δ 0.89 (t, J = 6.3 Hz, 3H), 1.29−1.50 (m, 19H), 1.63−1.75 (m, 1H), 2.86 (dd, J = 12.3, 7.5 Hz, 1H), 2.97 (dd, J = 10.6, 6.3 Hz, 1H), 3.57−3.61 (m, 2H), 3.65−3.69 (m, 1H), 3.75 (t, J = 6.5 Hz, 1H). ^{13}C NMR (CD$_3$OD, 100 MHz): δ 14.46, 23.74, 27.77, 30.48, 30.71, 30.75, 30.80, 30.89, 33.08, 35.29, 62.70, 63.25, 64.43, 79.58, 83.61. IR (KBr, cm^{-1}): 3290, 2922. HRMS (EI): m/z calcd for C$_{16}$H$_{33}$NO$_3$ (M$^+$) 287.2460, found 287.2461.

α-1-C-(4-Phenylbutyl)-LAB (1k). $[\alpha]_D^{24}$ = −35.7 (CH$_3$OH, c = 0.88). ^{1}H NMR (CD$_3$OD, 400 MHz): δ 1.39−1.53 (m, 3H), 1.62−1.74 (m, 3H), 2.62 (t, J = 7.7 Hz, 2H), 2.84−2.89 (m, 1H), 2.96−3.00 (m, 1H), 3.56−3.60 (m, 2H), 3.65−3.68 (m, 1H), 3.75 (t, J = 6.5 Hz, 1H). ^{13}C NMR (CD$_3$OD, 100 MHz): δ 27.33, 32.81, 34.93, 36.80, 62.76, 63.02, 64.53, 79.39, 83.40, 126.68, 129.28, 129.42, 143.78. IR (KBr, cm^{-1}): 3367, 3028, 2931, 2851. HRMS (EI): m/z calcd for C$_{15}$H$_{23}$NO$_3$ (M$^+$) 265.1678, found 265.1669.

α-1-C-(4-Methylpentyl)-LAB (1l). $[\alpha]_D^{24}$ = −44.8 (CH$_3$OH, c = 0.75). ^{1}H NMR (CD$_3$OD, 400 MHz): δ 0.89 (d, J = 6.8 Hz, 6H), 1.19−1.68 (m, 7H), 2.87−2.91 (m, 1H), 2.97−3.02 (m, 1H), 3.57−3.61 (m, 2H), 3.65−3.69 (m, 1H), 3.76 (t, J = 6.8 Hz, 1H). ^{13}C NMR (CD$_3$OD, 100 MHz): δ 22.97, 22.99, 25.56, 29.12, 35.33, 40.25, 62.88, 63.00, 64.55, 79.39, 83.40. IR (KBr, cm^{-1}): 3277, 2957, 2928, 2870. HRMS (EI): m/z calcd for C$_{11}$H$_{23}$NO$_3$ (M$^+$) 259.2147, found 259.2151.

Preparation of α-1-C-{(S)-1-Hydroxybutyl}-LAB (7) and α-1-C-{(R)-1-Hydroxybutyl}-LAB (8). (2R,5R)-Benzyl 2-{(Benzyloxy)methyl}-5-butyryl-2,5-dihydro-1H-pyrrole-1-carboxylate (10). To a suspension of the Mg chips (208 mg, 8.54 mmol) in THF (8.5 mL) was added 1-bromopropane (0.66 mL, 7.32 mmol) dropwise over 5 min at room temperature, and the reaction mixture was refluxed for 1 h. The resulting green-black solution was cooled to room temperature. To the reaction mixture was added a solution of Weinreb amide **9** (1.00 g, 2.44 mmol) in THF (5 mL), and the reaction was stirred for 3 h. The reaction mixture was poured into a two-layer mixture of Et$_2$O (15 mL) and saturated aqueous NH$_4$Cl (15 mL) at 0 °C. The aqueous layer was separated and extracted with EtOAc (30 mL). The combined organic layers were washed with saturated aqueous NaHCO$_3$ (15 mL) and brine (15 mL), dried over Na$_2$SO$_4$, and concentrated to yield a yellow oil. The residue was purified by flash chromatography (silica gel, 40 g, hexane/EtOAc = 4/1) to yield **10** (720 mg, 75%) as a pale yellow oil. $[\alpha]_D^{23}$ = +349.6 (CHCl$_3$, c = 1.96). ^{1}H NMR (CDCl$_3$, 400 MHz): (major) δ 0.75 (t, J = 7.2 Hz, 3H), 1.33−1.66 (m, 2H), 2.11 (dt, J = 17.4, 7.7 Hz, 1H), 2.23 (dt, J = 17.4, 7.7 Hz, 1H), 3.80 (dd, J = 9.2, 5.8 Hz, 1H), 3.91 (dd, J = 9.7, 2.9 Hz, 1H), 4.52 (d, J = 2.9 Hz, 1H), 4.88−4.91 (m, 1H), 5.10−5.14 (m, 3H), 5.66 (dt, J = 6.3, 1.9 Hz, 1H), 6.06 (dt, J = 6.3, 1.9 Hz, 1H), 7.23−7.38 (m, 10H); (minor) δ 0.89 (t, J = 7.2 Hz, 3H), 1.33−1.66 (m, 2H), 2.34 (dt, J = 17.4, 7.2 Hz, 1H), 2.46 (dt, J = 17.4, 7.2 Hz, 1H), 3.57 (dd, J = 9.2, 5.8 Hz, 1H), 3.74 (dd, J = 9.7, 2.9 Hz, 1H), 4.42 (d, J = 6.3 Hz, 1H), 4.78−4.82 (m, 2H), 4.99−5.02 (m, 3H), 5.72 (dt, J = 6.3, 1.9 Hz, 1H), 6.02 (dt, J = 6.3, 1.9 Hz, 1H), 7.23−7.38 (m, 10H). ^{13}C NMR (CDCl$_3$, 100 MHz): δ 13.55, 13.69, 16.48, 16.65, 38.94, 40.15, 64.56, 65.48, 67.18, 67.34, 69.12, 70.23, 73.24, 73.38, 74.29, 74.37, 124.87, 124.96, 126.96, 127.44, 127.46, 127.59, 127.64, 127.69, 128.12, 128.15, 128.20, 128.27, 128.34, 128.39, 128.47, 128.51, 128.55, 132.17, 132.22, 135.94, 136.22, 138.03, 138.20, 153.62, 206.44, 207.07. IR (neat, cm^{-1}): 2962, 2874, 1714.

HRMS (EI): *m/z* calcd for $C_{11}H_{23}NO_4$ (M+) 233.1627, found 233.1638.

(2R,5R)-Benzyl 2-((Benzyloxy)methyl)-5-{(S)-1-hydroxybutyl}-2,5-dihydro-1H-pyrrole-1-carboxylate (11). To a solution of ketone **10** (264 mg, 0.668 mmol) in Et_2O (4.5 mL) at 0 °C was added DIBAL-H (0.89 mL, 1.5 M in hexane, 1.34 mmol) dropwise over 5 min. After being stirred at this temperature for 2 h, the mixture was quenched by addition of EtOAc (5 mL) and 1 M aqueous potassium sodium tartrate (5 mL). The resulting mixture was stirred vigorously at room temperature for 2 h and then was extracted with EtOAc (2 × 15 mL). The combined organic layers were washed with brine (10 mL) and dried over anhydrous Na_2SO_4. Filtration and evaporation in vacuo furnished the crude product, which was purified by column chromatography (silica gel, 15 g, hexane/EtOAc = 3/1 → hexane/EtOAc = 2/1) to give **11** (172 mg, 65%) as a colorless oil and **12** (47.8 mg, 18%) as a colorless oil. $[\alpha]_D^{23}$ = +227.2 (CHCl₃, *c* = 0.98). ¹H NMR (CDCl₃, 400 MHz): (major) δ 0.90 (t, *J* = 7.2 Hz, 3H), 1.20−1.34 (m, 4H), 3.56 (dd, *J* = 9.2, 5.8 Hz, 1H), 3.71 (dd, *J* = 9.2, 2.9 Hz, 1H), 3.84−3.88 (m, 1H), 4.09 (d, *J* = 9.7 Hz, 1H), 4.34−4.49 (m, 2H), 4.61−4.64 (m, 1H), 4.86−4.87 (m, 1H), 5.08 (d, *J* = 2.4 Hz, 2H), 5.70 (dt, *J* = 6.8, 1.9 Hz, 1H), 5.89 (dt, *J* = 6.8, 1.9 Hz, 1H), 7.22−7.35 (m, 10H); (minor) δ 0.88 (t, *J* = 7.2 Hz, 3H), 1.20−1.34 (m, 4H), 3.52−3.58 (m, 1H), 3.67−3.721 (m, 1H), 3.84−3.88 (m, 1H), 4.09 (m, 1H), 4.34−4.49 (m, 2H), 4.61−4.64 (m, 1H), 4.86−4.87 (m, 1H), 5.03−5.09 (m, 2H), 5.70−5.72 (m, 1H), 5.88−6.01 (m, 1H), 7.22−7.35 (m, 10H). ¹³C NMR (CDCl₃, 100 MHz): δ 14.11, 19.46, 33.50, 65.35, 67.38, 70.27, 72.09, 72.33, 73.16, 127.42, 127.52, 127.65, 128.09, 128.16, 128.21, 128.30, 128.38, 128.54, 129.55, 136.12, 138.12, 155.73. IR (neat, cm⁻¹): 3430, 2957, 1683. HRMS (EI): *m/z* calcd for $C_{24}H_{29}NO_4$ (M+) 395.2097, found 395.2097.

(2S,3S,4S,5S)-Benzyl-2-{(benzyloxy)methyl}-3,4-dihydroxy-5-{(S)-1-hydroxybutyl}pyrrolidine-1-carboxylate (14). To a vial containing **11** (122 mg, 0.308 mmol) were added CH_3CN (3.1 mL) and 4 × 10⁻⁴ M ethylenediaminetetraacetic acid in H_2O (2.1 mL). The solution was cooled to 0 °C, and 1,1,1-trifluoroacetone (345 mg, 3.08 mmol) was added. A mixture of solid Oxone (947 mg, 1.54 mmol) and $NaHCO_3$ (245 mg, 2.31 mmol) was added in four portions over 45 min. The reaction was stirred for 2 h at 0 °C, then diluted with 5 mL of H_2O, and extracted with EtOAc (2 × 15 mL). The organic layers were combined and dried over anhydrous Na_2SO_4. Filtration and evaporation in vacuo furnished the crude product, which was purified by column chromatography (silica gel, 6 g, Et_2O) to provide a mixture of epoxides **13** (105 mg, 83%) as a colorless oil. Trifluoroacetic acid (0.25 mL, 3.37 mmol) was added to a solution of the epoxides **13** (102 mg, 0.248 mmol) in THF/H_2O (3/2, 2.5 mL). After being stirred at 70 °C for 12 h, the reaction mixture was cooled to room temperature, quenched by addition of saturated aqueous $NaHCO_3$ (5 mL), and extracted with EtOAc (3 × 5 mL). The combined organic layers were washed with brine (5 mL) and dried over anhydrous Na_2SO_4. Filtration and evaporation in vacuo furnished the crude product, which was purified by column chromatography (silica gel, 5 g, hexane/EtOAc = 2/1 → hexane/EtOAc = 1/1) to yield diol **14** (100 mg, 93%) as a colorless oil. $[\alpha]_D^{22}$ = −+57.8 (CHCl₃, *c* = 1.21). ¹H NMR (CDCl₃, 400 MHz, ca.1:1 mixture): δ 0.86 (t, *J* = 6.8 Hz, 3H), 0.97 (t, *J* = 6.8 Hz, 3H), 1.25−1.61 (m, 8H), 3.50−3.58 (m, 2H), 3.84−4.15 (m, 10H), 4.28−4.57 (m, 6H), 4.76−5.17 (m, 6H), 7.20−7.35 (m, 10H). ¹³C NMR (CDCl₃, 100 MHz): δ 14.03, 14.30, 19.46, 19.62, 36.61, 36.69, 67.32, 67.38, 67.76, 67.81, 68.48, 69.26, 70.84, 73.08, 73.65, 73.88, 74.09, 76.03, 77.64, 79.73, 80.69, 128.15, 128.22, 128.26, 128.52, 128.54, 128.55, 128.64, 128.86, 128.92, 128.99, 136.37, 136.45, 136.68, 136. 82, 154.80, 154.83. IR (neat, cm⁻¹): 3390, 2958, 2927, 1683. HRMS (EI): *m/z* calcd for $C_{24}H_{31}NO_6$ (M+) 429.2151, found 429.2146.

α-1-C-{(S)-1-Hydroxybutyl}-LAB (7). Pd/C (5% Pd, 9.8 mg, 10 wt %) was added to a stirred solution of diol **14** (98.4 mg, 0.229 mmol) in MeOH (2.3 mL) and concentrated HCl (3 drops). The reaction mixture was stirred for 10 h under a balloon of H_2. The reaction mixture was filtered through Celite (eluting with MeOH) and concentrated in vacuo. The product was purified by flash chromatography (silica gel, 3 g, Et_2O/MeOH/25% NH₃(aq) = 80/

20/1 →Et_2O/MeOH/25% NH₃(aq) = 0/100/2) to yield **7** (32.0 mg, 68%) as a white amorphous solid. $[\alpha]_D^{22}$ = −17.1 (CH₃OH, *c* = 1.32). ¹H NMR (CD₃OD, 400 MHz): δ 0.97 (t, *J* = 7.2 Hz, 3H), 1.36−1.64 (m, 4H), 3.37−3.40 (m, 2H), 3.77−3.90 (m, 3H), 3.97 (t, *J* = 6.8 Hz, 1H), 4.23 (t, *J* = 6.8 Hz, 1H). ¹³C NMR (CD₃OD, 100 MHz): δ 14.24, 19.96, 36.67, 58.62, 64.77, 66.01, 69.72, 75.09, 76.64. IR (neat, cm⁻¹): 3350, 2962. HRMS (FAB): *m/z* calcd for $C_9H_{20}NO_4$ (M + H+) 206.1392, found 206.1394.

(2R,5R)-Benzyl 2-{(Benzyloxy)methyl}-5-{(R)-1-hydroxybutyl}-2,5-dihydro-1H-pyrrole-1-carboxylate (12). To a solution of ketone **10** (360 mg, 0.915 mmol) in MeOH (6 mL) at 0 °C was added $NaBH_4$ (69.2 mg, 1.83 mmol). After being stirred at this temperature for 1 h, the mixture was quenched by addition of H_2O (5 mL). The resulting mixture was extracted with EtOAc (2 × 25 mL). The combined organic layers were washed with brine (15 mL) and dried over anhydrous Na_2SO_4. Filtration and evaporation in vacuo furnished the crude product, which was purified by column chromatography (silica gel, 15 g, hexane/EtOAc = 3/1 → hexane/EtOAc = 2/1) to give **11** (87.5 mg, 24%) as a colorless oil and **12** (183 mg, 51%) as a colorless oil. $[\alpha]_D^{22}$ = +234.6.0 (CHCl₃, *c* = 0.80). ¹H NMR (CDCl₃, 400 MHz): (major) δ 0.91 (t, *J* = 6.8 Hz, 3H), 1.10−1.60 (m, 4H), 3.54 (dd, *J* = 9.2, 6.3 Hz, 1H), 3.68 (dd, *J* = 9.2, 2.4 Hz, 1H), 3.94 (br s, 1H), 4.34−4.43 (m, 3H), 4.51−4.70 (m, 2H), 5.07 (d, *J* = 6.8 Hz, 2H), 5.82−5.88 (m, 2H), 7.22−7.36 (m, 10H); (minor) δ 0.81 (t, *J* = 6.8 Hz, 3H), 1.10−1.60 (m, 4H), 3.81−3.91 (m, 2H), 4.16 (br s, 1H), 4.51−4.70 (m, 5H), 5.03−5.22 (m, 2H), 5.82−5.96 (m, 2H), 7.22−7.36 (m, 10H). ¹³C NMR (CDCl₃, 100 MHz): δ 14.11, 18.51, 19.08, 35.13, 64.83, 65.77, 66.88, 67.38, 70.30, 72.07, 73.16, 73.27, 74.11, 126.76, 127.11, 127.39, 127.43, 127.65, 128.22, 128.23, 128.30, 128.39, 128.54, 129.05, 136.08, 138.13, 155.89, 155.90. IR (neat, cm⁻¹): 3435, 2933, 2871, 1682. HRMS (EI): *m/z* calcd for $C_{24}H_{29}NO_4$ (M+) 395.2097, found 395.2097.

(2S,3S,4S,5S)-Benzyl 2-{(Benzyloxy)methyl}-3,4-dihydroxy-5-{(R)-1-hydroxybutyl}pyrrolidine-1-carboxylate (16). To a vial with **12** (155 mg, 0.392 mmol) were added CH_3CN (3.9 mL) and 4 × 10⁻⁴ M ethylenediaminetetraacetic acid in H_2O (2.6 mL). The solution was cooled to 0 °C, and 1,1,1-trifluoroacetone (439 mg, 3.08 mmol) was added. A mixture of solid Oxone (1.21 g, 1.96 mmol) and $NaHCO_3$ (312 mg, 2.94 mmol) was added in four portions over 45 min. The reaction was stirred for 2 h at 0 °C, then diluted with 5 mL of H_2O, and extracted with EtOAc (2 × 15 mL). The organic layers were combined and dried over anhydrous Na_2SO_4. Filtration and evaporation in vacuo furnished the crude product, which was purified by column chromatography (silica gel, 6 g, Et_2O) to provide a mixture of epoxides **15** (129 mg, 80%) as a colorless oil. Trifluoroacetic acid (0.30 mL, 4.04 mmol) was added to a solution of the epoxides **13** (125 mg, 0.304 mmol) in THF/H_2O (3/2, 3.0 mL). After being stirred at 70 °C for 12 h, the reaction mixture was cooled to room temperature, quenched by addition of saturated aqueous $NaHCO_3$ (5 mL), and extracted with EtOAc (3 × 5 mL). The combined organic layers were washed with brine (5 mL) and dried over anhydrous Na_2SO_4. Filtration and evaporation in vacuo furnished the crude product, which was purified by column chromatography (silica gel, 5 g, hexane/EtOAc = 2/1 → hexane/EtOAc = 1/1) to yield diol **14** (21.0 mg, 16%) as a colorless oil. $[\alpha]_D^{20}$ = +77.3 (CHCl₃, *c* = 0.19). ¹H NMR (CDCl₃, 400 MHz): (major) δ 0.94 (t, *J* = 6.8 Hz, 3H), 1.33−1.88 (m, 4H), 3.45−3.57 (m, 1H), 3.67−4.09 (m, 5H), 4.29−4.37 (m, 1H), 4.45−4.59 (m, 2H), 5.02−5.17 (m, 2H), 7.18−7.35 (m, 10H); (minor) δ 0.78 (t, *J* = 6.8 Hz, 3H), 1.33−1.88 (m, 4H), 3.45−3.57 (m, 1H), 3.67−4.09 (m, 5H), 4.29−4.37 (m, 1H), 4.45−4.59 (m, 2H), 5.02−5.17 (m, 2H), 7.18−7.35 (m, 10H). ¹³C NMR (CDCl₃, 100 MHz): δ 13.78, 13.99, 19.08, 19.30, 29.70, 38.19, 67.11, 67.40, 67.59, 68.61, 68.77, 71.18, 72.53, 73.50, 73.74, 74.49, 74.97, 79.62, 80.55, 81.07, 81.68, 127.95, 128.26, 128.35, 128.54, 128.60, 135.99, 136.38, 136.67, 155.16, 156.61. IR (neat, cm⁻¹): 3390, 2958, 2927, 1674. HRMS (EI): *m/z* calcd for $C_{24}H_{31}NO_6$ (M+) 429.2151, found 429.2150.

α-1-C-{(R)-1-Hydroxybutyl}-LAB (8). Pd/C (5% Pd, 2.1 mg, 10 wt %) was added to a stirred solution of diol **16** (20.6 mg, 0.0480 mmol) in MeOH (1.0 mL) and concentrated HCl (1 drop). The reaction mixture was stirred for 10 h under a balloon of H_2. The reaction

mixture was filtered through Celite (eluting with MeOH) and concentrated in vacuo. The product was purified by flash chromatography (silica gel, 2 g, Et_2O/MeOH/25% NH_3(aq) = 80/20/1 → Et_2O/MeOH/25% NH_3(aq) = 0/100/2) to yield **8** (9.30 mg, 94%) as a white amorphous solid. $[\alpha]_D^{22}$ = −11.6 (CH_3OH, c = 0.10). ^1H NMR (CD_3OD, 400 MHz): δ 0.97 (t, J = 7.2 Hz, 3H), 1.39−1.57 (m, 4H), 3.20−3.23 (m, 1H), 3.34−3.38 (m, 1H), 3.75−3.88 (m, 3H), 3.97−4.02 (m, 2H), 4.88 (br s, 1H). ^{13}C NMR (CD_3OD, 100 MHz): δ 14.16, 19.64, 37.61, 58.98, 64.92, 67.73, 68.68, 76.16, 76.43. IR (neat, $cm^{−1}$): 3367, 2931. HRMS (FAB): m/z calcd for $C_9H_{20}NO_4$ (M + H^+) 206.1392, found 206.1384.

N-Butyl-α-1-C-butyl-LAB (17). Sodium borocyanohydride (9.9 mg, 0.15 mmol) and butyraldehyde (30 μL, 0.32 mmol) were added to the solution of (2S,3S,4S,5S)-2-butyl-5-(hydroxymethyl)pyrrolidine-3,4-diol (19 mg, 0.10 mmol) in MeOH (2.0 mL) at 0 °C, and the resulting solution was stirred for 2 h at the same temperature. Then the solvent was removed under reduced pressure. The residue was purified by silica gel SiO_2 column chromatography to obtain **17** (11.2 mg, 46%). $[\alpha]_D^{20}$ = +36.9 ($CHCl_3$, c = 1.01). ^1H NMR (400 MHz, $CDCl_3$): δ 0.87−0.94 (m, 6H), 1.25−1.50 (m, 9H), 1.58−1.67 (m, 1H), 2.57−2.72 (m, 2H), 2.85 (br s, 1H), 3.07 (br d, J = 10.1 Hz, 1H), 3.72−3.81 (m, 2H), 3.86 (br s, 1H), 4.11 (br d, J = 3.4 Hz, 1H), 4.20 (br s, 3H). ^{13}C NMR (100 MHz, $CDCl_3$): δ 13.92, 14.03, 20.58, 22.85, 25.24, 28.36, 29.50, 46.56, 58.90, 67.74, 69.45, 79.97, 80.42. IR (neat) $cm^{−1}$ 3391, 2959, 2873, 2344, 2173. HRMS (EI): m/z calcd for $C_{13}H_{27}NO_3$ (M^+) 245.1991, found 245.1980.

(5S,6R,7S,7aR)-5,7-Dibutyltetrahydro-6-hydroxypyrrolo[1,2-c]-oxazol-3(1H)-one (19). CuI (84.6 mg, 0.44 mmol) was dried under reduced pressure, and Et_2O (0.7 mL) was added under an argon atmosphere. The solution was cooled at 0 °C, and n-BuLi (1.6 M hexane solution, 0.55 mL, 0.50 mmol) was added. The solution was stirred until the yellow color disappeared. The resulting solution was utilized as the ether solution of n-Bu_2CuLi. The prepared ether solution of n-Bu_2CuLi was added to the solution of **5c** (43.2 mg, 0.22 mmol) in Et_2O (0.7 mL) at −20 °C under an argon atmosphere. The solution was stirred until the starting material disappeared on TLC. Then a saturated aqueous solution of NH_4Cl was added to quench the reaction. The resulting mixture was extracted with CH_2Cl_2 and dried over Na_2SO_4. The solvent was removed under reduced pressure, and the residue was purified by silica gel column chromatography (Et_2O) to afford **19** (13 mg, 23%). $[\alpha]_D^{24}$ = +11.5 ($CHCl_3$, c = 1.30). ^1H NMR (400 MHz, $CDCl_3$): δ 0.88−0.94 (m, 6H), 1.20−1.55 (m, 10H), 1.60−1.69 (m, 2H), 1.83−1.88 (m, 1H), 3.57−3.74 (m, 2H), 3.72 (dd, J = 7.7, 5.3 Hz, 1H), 4.19 (dd, J = 9.2, 3.9 Hz, 1H), 4.47 (t, J = 8.7 Hz, 1H). ^{13}C NMR (100 MHz, $CDCl_3$): δ 13.85, 13.98, 22.54, 22.94, 28.24, 30,10, 30.50, 33.82, 52.85, 62.13, 66.27, 67.47, 84.92, 161.30. IR (KBr, $cm^{−1}$): 3426, 1733, 1398, 1227. HRMS (EI): m/z calcd for $C_{14}H_{25}NO_3$ (M^+) 255.1843, found 255.1832.

(2S,3R,4S,5R)-2,4-Dibutyl-5-(hydroxymethyl)pyrrolidin-3-ol (18). To the solution of **19** (13 mg, 0.051 mmol) in EtOH (0.4 mL) were added H_2O (0.2 mL) and NaOH (20 mg, 0.5 mmol) at room temperature. The solution was refluxed at 100 °C for 1 h. Then the solvent was removed under reduced pressure. The residue was purified by silica gel SiO_2 column chromatography (MeOH) to obtain **18** (4.4 mg, 38%). $[\alpha]_D^{20}$ = −15.6 (CH_3OH, c = 0.44). ^1H NMR (400 MHz, CD_3OD): δ 0.89−0.96 (m, 6H), 1.25−1.80 (m, 13H), 2.90−3.05 (m, 2H), 3.43 (t, J = 8.2 Hz, 1H), 3.55 (dd, J = 11.6, 7.2 Hz, 1H), 3.64 (dd, J = 11.6, 3.7 Hz, 1H). ^{13}C NMR (100 MHz, CD_3OD): δ 14.28, 14.32, 23.81, 24.01, 29.96, 30.79, 30.89, 33.10, 33.28, 35.17, 63.87, 64.04, 64.13, 82.38. IR (KBr, $cm^{−1}$): 3375, 1561, 1467. HRMS (EI): m/z calcd for $C_{14}H_{25}NO_3$ (M^+) 229.2042, found 229.2049.

Assay of Enzyme Inhibition. Brush border membranes were prepared from the rat small intestine according to the method of Kessler et al.[63] and were assayed at pH 5.8 for rat intestinal maltase, isomaltase, sucrase, cellobiase, and lactase using the appropriate disaccharides as substrates. For rat intestinal maltase activities, the reaction mixture contained 25 mM maltose and the appropriate amount of enzyme, and the incubations were performed for 10−30 min at 37 °C. The reaction was stopped by heating at 100 °C for 3 min. After centrifugation (600g, 10 min), 0.05 mL of the resulting reaction mixture was added to 3 mL of the glucose CII-test reagent (Wako Pure Chemical Industries, Osaka, Japan). The absorbance at 505 nm was measured to determine the amount of the released D-glucose. Kinetic parameters were determined by the double-reciprocal-plot method of Lineweaver−Burk at increasing concentrations of the appropriate maltose.

Glycoblotting. The human hepatocellular carcinoma HepG2 cell line was obtained from the European Collection of Cell Cultures (ECACC 85011430). Cells were cultured in low-glucose Dulbecco's modified Eagle's medium (Invitrogen, Carlsbad, CA), supplemented with 10% fetal calf serum (Invitrogen), and maintained in a humidified incubator at 37 °C with 5% CO_2. N-Linked oligosaccharide analysis was performed on HepG2 cells after treatment for 48 h with miglitol or α-1-C-butyl-LAB, which gave additional N-linked oligosaccharide in the MALDI-TOF MS profiles derived from HepG2 homogenates (Figure 3b,c) in comparison to untreated controls (Figure 3a). Cell pellets were homogenized in 0.5% Triton X-100 solution. The solubilized proteinaceous materials were reduced by dithiothreitol (DTT) at 60 °C for 30 min followed by alkylation with 10 μL of 123 mM iodoacetamide (IAA) by incubation in the dark at 25 °C for 60 min. The mixture was then treated with 10 μL of 40 units/μL trypsin at 37 °C for 60 min, followed by heat inactivation of the enzyme at 90 °C for 10 min. After being cooled to room temperature, N-glycans were enzymatically released from trypsin-digested glycopeptides by incubation with 5 units of PNGase F (Roche Applied Science, Switzerland) at 37 °C for 16 h. PNGase F-treated samples were dropped onto BlotGlyco beads (Sumitomo Bakelite Co., Tokyo, Japan) in a filter plate, and this was followed by addition of 2% acetic acid/acetonitrile. After incubation at 80 °C for 60 min to covalently ligate glycans onto the beads, the beads were washed with 2 M guanidine hydrochloride, distilled water, and 1% triethylamine/methanol to remove nonspecifically bound impurities. After washing, the beads were treated with 10% acetic anhydride/methanol for 30 min at ambient temperature to quench the hydrazide groups. The beads were then washed serially with 10 mM hydrochloric acid, distilled water, methanol, and dimethyl sulfoxide (DMSO). On-bead methyl esterification was performed by the reaction with 500 mM 1-methyl-3-p-tolyltriazene/DMSO solution at 60 °C for 60 min. After the beads were washed with methanol and distilled water, the trapped glycans were finally released and recovered as N^α-((aminooxy)acetyl)-tryptophanylarginine methyl ester (aoWR) derivatives by adding 20 mM aoWR and 2% acetic acid/acetonitrile and incubated at 80 °C for 1 h. The resulting aoWR-labeled glycans were recovered by washing the beads with distilled water, and the collected solution was further purified with a solid-phase extraction column (Cleanup column, Sumitomo Bakelite Co.) to remove the excess aoWR. The purified solution was mixed with 2,5-dihydroxybenzoic acid solution and subsequently subjected to MALDI-TOF analysis.

MALDI-TOF MS Analysis. All measurements were performed with an Autoflex III TOF/TOF mass spectrometer equipped with a reflector and controlled by the FlexControl 3.0 software package (Bruker Daltonics GmbH, Bremen, Germany), according to a general protocol reported previously.[51] The peaks were detected generally as a formula of $[M + H]^+$ ions. In MALDI-TOF MS reflector mode, ions generated by a Smartbeam (pulsed UV nitrogen laser, λ = 337 nm, 5 Hz) were accelerated to a kinetic energy of 23.5 kV. Masses were automatically annotated by using FlexAnalysis 2.0. External calibration of MALDI mass spectra was carried out using singly charged monoisotopic peaks of a mixture of human angiotensin II (m/z 1046.542), bombesin (m/z 1619.823), adrenocorticotropin (18−39) (m/z 2465.199), and somatostatin 28 (m/z 3147.472). All measurements were performed as follows: 1 mL of the sample solution was mixed with 1 mL of 2,5-dihydroxybenzoic acid (10 mg/mL in 30% ACN), and 1 mL of the resulting mixture was subjected to MALDI-TOF mass analysis. Structural identification of glycans was performed by MS analysis and the use of a database for glycan structures[64] (http://web.expasy.org/glycomod/).

Disaccharide Loading Test. The animal experimental protocols in this study were approved by the Animal Experiments Committee of the University of Toyama (S-2010 UH-2). Male ddY mice (29−33 g)

after an overnight fast were used for acute disaccharide loading tests. Maltose (2.5 g/kg of body weight) or sucrose (2.5 g/kg of body weight) as well as the inhibitor, miglitol, was dissolved in 0.9% NaCl solution and administered to the mice via a stomach tube. A control group was loaded with saline only. Blood samples for glucose measurements were obtained from the tail vein at 0, 15, 30, 60, and 120 min after disaccharide loading. The blood glucose levels were measured by a portable kit, StatStrip Xpress (Nova Biomedical Co. Ltd., Waltham, MA). The AUC over a period of 60 min after disaccharide loading was calculated by the trapezoidal method.

Homology Modeling of the Rat *N*-Terminal Catalytic Domain of ntMGAM. The α-glucosidase activities are associated with two small intestinal membrane-bound enzymes: maltase-glucoamylase and sucrase-isomaltase. The *N*-terminal catalytic domain of maltase-glucoamylase (ntMGAM) has a preference for short linear α-1,4 oligosaccharides such as maltose.[65] To investigate the inhibitory activity of α-1-*C*-butyl-LAB on the hydrolysis of maltose in rats, we first constructed a three-dimensional model of rat ntMGAM using homology modeling with Prime 1.5 (Schrödinger, Portland, OR), because the three-dimensional structure of rat ntMGAM has not been determined experimentally. The amino acid sequence of rat ntMGAM was taken from the UniProtKB-Swiss-Prot database (accession number Q6P7A9). Sequences homologous to the rat ntMGAM against the Protein Data Bank (PDB) were performed using a BLAST search, and the three-dimensional structures of human ntMGAM were subsequently found (sequence identity between rat ntMGAM and human ntMGAM, 45%). Four representative structures of human ntMGAM were obtained by clustering 12 three-dimensional structures of human ntMGAM taken from the PDB on the basis of side chain structures around the ligand (PDB IDs 2QLY, 2QMJ, 3CTT, and 3L4W). Using four template structures of human ntMGAM, we constructed the homology models of rat ntMGAM. The stereochemical quality evaluation using PROCHECK indicated that the four homology models are reasonable.[66]

Docking Studies of α-1-*C*-Butyl-LAB, α-1-*C*-Butyl-DNJ, and Miglitol with Rat ntMGAM. Docking calculations of α-1-*C*-butyl-LAB, α-1-*C*-butyl-DNJ, and miglitol with the homology models of rat ntMGAM were carried out using the standard precision mode for Glide 5.5 in the Schrödinger suite. The top three poses ranked with GlideScore[67] were minimized by an OPLS2005 force field, and the docking model that exhibited the most stable interaction energy was then selected as the best model. The binding free energies between rat ntMGAM and the compounds were calculated accurately by combining an OPLS2005 force field with the GB/SA continuum solvation model to include the effect of solvent.[68] The binding energy was estimated as follows: $\Delta E = E_{complex} - (E_{protein} - E_{ligand})$. Here, $E_{complex}$, $E_{protein}$, and E_{ligand} are the molecular mechanics energies of the complex structure, the protein structure, and the ligand structure, respectively.

Docking Studies of α-1-*C*-Butyl-LAB and α-1-*C*-Butyl-DNJ with Human β-Glucocerebrosidase. The docking calculations of α-1-*C*-butyl-LAB and α-1-*C*-butyl-DNJ with β-glucocerebrosidase were carried out using the X-ray of human β-glucocerebrosidase (PDB ID 2NSX) and Induced Fit Docking[69] in the Schrödinger package. For the initial docking process of the Induced Fit Docking, van der Waals (vdW) radii of both the ligand and the receptor were scaled to 0.5 to soften the surfaces of the protein and the ligand, and Asn396 was temporarily mutated to alanine because multiple X-ray structures showed that the orientation of the side chain of Asn396 changes. The ligands were then redocked back into the new receptor using the default vdW radii scaling (1.0 receptor, 0.8 ligand), and Asn396 mutated to alanine was restored in the final docking. The standard precision mode was used in the docking analysis. IFDScore was the sum of the docking energy, receptor strain, and solvation terms. Finally, the top pose ranked by IFDScore was minimized by an OPLS2005 force field.

■ ASSOCIATED CONTENT

ⓢ Supporting Information
General experimental protocols and ^{1}H and ^{13}C NMR spectra of the compounds. This material is available free of charge via the Internet at http://pubs.acs.org.

■ AUTHOR INFORMATION

Corresponding Author
*Phone: +81-76-434-7868 (A.K.); +81-22-727-0144 (H.T.). E-mail: kato@med.u-toyama.ac.jp (A.K.); takahata@tohoku-pharm.ac.jp (H.T.).

Notes
The authors declare no competing financial interest.

■ ABBREVIATIONS USED

LAB, 1,4-dideoxy-1,4-imino-L-arabinitol; DAB, 1,4-dideoxy-1,4-imino-D-arabinitol; DNJ, 1-deoxynojirimycin; DMDP, (2*R*,5*R*)-bis(dihydroxymethyl)-(3*R*,4*R*)-dihydroxypyrrolidine; IC$_{50}$, concentration of compound required to induce 50% inhibition; ER, endoplasmic reticulum; MALDI-TOF MS, matrix-assisted laser desorption ionization time-of-flight mass spectrometry; AUC, area under the curve; ntMGAM, *N*-terminal catalytic domain of maltase-glucoamylase; AAA, asymmetric allylic alkylation; RCM, ring-closing metathesis

■ REFERENCES

(1) Tuomilehto, J.; Lindström, J.; Eriksson, J. G.; Valle, T. T.; Hämäläinen, H.; Ilanne-Parikka, P.; Keinänen-Kiukaanniemi, S.; Laakso, M.; Louheranta, A.; Rastas, M.; Salminen, V.; Uusitupa, M. (for the Finnish Diabetes Prevention Study Group). Prevention of type 2 diabetes mellitus by changes in lifestyle among subjects with impaired glucose tolerance. *N. Engl. J. Med.* **2001**, *344*, 1343−1350.

(2) Lyssenko, V; Jonsson, A.; Almgren, P.; Pulizzi, N.; Isomaa, B.; Tuomi, T.; Berglung, G.; Alshuler, D.; Nilsson, P.; Groop, L. Clinical risk factors, DNA variants, and the development of type 2 diabetes. *N. Engl. J. Med.* **2008**, *359*, 2220−2232.

(3) McCarthy, M. I. Genomics, type 2 diabetes, and obesity. *N. Engl. J. Med.* **2010**, *363*, 2339−2350.

(4) Shaw, J. E.; Sicree, R. A.; Zimmet, P. Z. Global estimates of the prevalence of diabetes for 2010 and 2030. *Diabetes Res. Clin. Pract.* **2010**, *87*, 4−14.

(5) Gerich, J. E. Clinical significance, pathogenesis, and management of postprandial hyperglycemia. *Arch. Intern. Med.* **2003**, *163*, 1306−1316.

(6) UK Prospective Diabetes Study Group.. Intensive blood-glucose control with sulphonylureas or insulin compared with conventional treatment and risk of complications in patients with type 2 diabetes (UKPDS 33). *Lancet* **1998**, *352*, 837−853.

(7) UK Prospective Diabetes Study Group.. Effect of intensive blood-glucose control with metformin on complications in overweight patients with type 2 diabetes (UKPDS 34). *Lancet* **1998**, *352*, 854−865.

(8) Stratton, I. M.; Adler, A. I.; Neil, H. A. W.; Matthws, D. R.; Manley, S. E.; Cull, C. A.; Hadden, D.; Turner, R. C.; Holman, R. R. Association of glycaemia with macrovascular and microvascular complications of type 2 diabetes (UKPDS 35): prospective observational study. *BMJ [Br. Med. J.]* **2000**, *321*, 405−412.

(9) Hanefeld, M.; Cagatay, M.; Petrowitsch, T.; Neuse, D.; Petzinna, D.; Rupp, M. Acarbose reduces the risk for myocardial infarction in type 2 diabetic patients: meta-analysis of seven long-term studies. *Eur. Heart J.* **2004**, *25*, 10−16.

(10) Coutinho, M.; Gerstein, H. C; Wang, Y.; Yusuf, S. The relationship between glucose and incident cardiovascular events. A metaregression analysis of published data from 20 studies of 95,783 individuals followed for 12.4 years. *Diabetes Care* **1999**, *22*, 233−240.

(11) Bonora, E.; Muggeo, M. Postprandial blood glucose as a risk factor for cardiovascular disease in type II diabetes: the epidemiological evidence. *Diabetologia* **2001**, *44*, 2107−2114.

(12) Ceriello, A. Postprandial hyperglycemia and diabetes complications: is it time to treat? *Diabetes* **2005**, *54*, 1−7.

(13) Iwasa, M.; Yamada, Y.; Kobayashi, H.; Yasuda, S.; Kawamura, I.; Sumi, S.; Shiraki, T.; Yamaki, T.; Ushikoshi, H.; Hattori, A.; Aoyama, T.; Nishigaki, K.; Takemura, G.; Fujiwara, H; Minatoguchi, S. Both stimulation of GLP-1 receptors and inhibiton of glycogenolysis additively contribute to a protective effect of oral miglitol against ishaemia-reperfusion injury in rabbits. *Br. J. Pharmacol.* **2011**, *164*, 119−131.

(14) Asano, N.; Nash, R. J.; Molyneux, R. J.; Fleet, G. W. J. Sugar-mimic glycosidase inhibitors: natural occurrence, biological activity and prospects for therapeutic application. *Tetrahedron: Asymmetry* **2000**, *11*, 1645−1680.

(15) Sim, L.; Jayakanthan, K.; Mohan, S.; Nasi, R.; Johnston, B. D.; Pinto, B. M.; Rose, D. R. New glucosidase inhibitors from an ayurvedic herbal treatment for type 2 diabetes: structures and inhibition of human intestinal maltase-glucoamylase with compounds from *Salacia reticulata*. *Biochemistry* **2010**, *49*, 443−451.

(16) Eskandari, R.; Jones, K.; Rose, D. R.; Pinto, B. M. Selectivity of 3′-O-methylponkoranol for inhibition of N- and C-terminal maltase glucoamylase and sucrase isomaltase, potential therapeutics for digestive disorders or their sequelae. *Bioorg. Med. Chem. Lett.* **2011**, *21*, 6491−6494.

(17) Ogawa, S. Synthetic studies on glycosidase inhibitors composed of 5a-carba-sugars. *Carbohydrate Mimics: Concepts and Methods*; Chapleur, Y., Ed.; Wiley-VCH: Weinheim, Germany, 1998; pp 87−106.

(18) Horii, S.; Iwasa, T.; Mizuta, E.; Kameda, Y. Studies on validamycins, new antibiotics. VI. Validamine, hydroxyvalidamine and validatol, new cyclitols. *J. Antibiot.* **1971**, *24*, 59−63.

(19) Kameda, Y.; Asano, N.; Yoshikawa, M.; Matsui, K. Valienamine as an α-glucosidase inhibitor. *J. Antibiot.* **1980**, *33*, 1575−1576.

(20) Kameda, Y.; Asano, N.; Yoshikawa, M.; Takeuchi, M.; Yamaguchi, T.; Matsui, K. Valiolamine, a new α-glucosidase inhibiting aminocyclitol produced by *Streptomyces hygroscopicus*. *J. Antibiot.* **1984**, *37*, 1301−1307.

(21) Horii, S; Fukase, H.; Matsuo, T.; Asano, N.; Matsui, K. Synthesis and α-D-glucosidase inhibitory activity of N-substituted valiolamine derivatives as potential oral antidiabetic agents. *J. Med. Chem.* **1986**, *29*, 1038−1046.

(22) Kato, A.; Kato, N.; Kano, E.; Adachi, I.; Ikeda, K.; Yu, L.; Okamoto, T.; Banba, Y.; Ouchi, H.; Takahata, H.; Asano, N. Biological properties of D- and L-1-deoxyazasugars. *J. Med. Chem.* **2005**, *48*, 2036−2044.

(23) Junge, B.; Matzke, M.; Stltefuss, J. In *Handbook of Experimental Pharmacology*; Kuhlmann, J., Puls, W., Eds.; Springer-Verlag: New York, 1996; Vol. *119*, p 411.

(24) Cauderay, M.; Tappy, L.; Temler, E.; Jequier, E.; Hillebrand, I.; Felber, J. P. Effect of α-glucohydrolase inhibitors (Bay m1099 and Bay o1248) on sucrose metabolism in normal men. *Metabolism* **1986**, *35*, 472−477.

(25) Madar, Z.; Olefsky, J. Effect of the α-glucosidase inhibitor Bay-O-1248 on the metabolic response of nondiabetic and diabetic rats to a high-carbogydrate diet. *Am. J. Clin. Nutr.* **1986**, *44*, 206−211.

(26) Taylor, R. H.; Barker, H. M.; Bowey, E. A.; Canfield, J. E. Regulation of absorption of dietary carbohydrate in man by two new glycosidase inhibitors. *Gut* **1986**, *27*, 1471−1478.

(27) Wisselaar, H. A.; van Dongen, J. M.; Reuser, A. J. Effects of N-hydroxyethyl-1-deoxynojirimycin (BAY m 1099) on the activity of neutral- and acid α-glucosidases in human fibroblasts and HepG2 cells. *Clin. Chim. Acta* **1989**, *182*, 41−52.

(28) Putter, J. In *Enzyme Inhibitors*; Brodech, E., Ed.; Verlag Chemie: Weinheim, Germany, 1980; p 139.

(29) Joubert, P. H.; Venter, H. L.; Foukaridis, G. N. The effect of miglitol and acarbose after an oral glucose load: a novel hypoglycaemic mechanism? *Br. J. Clin. Pharmacol.* **1990**, *30*, 391−396.

(30) Bischoff, H. Pharmacology of α-glucosidase inhibition. *Eur. J. Clin. Invest.* **1994**, *24*, 3−10.

(31) Arh, H. J.; Boberg, M; Brendei, E.; Krause, H. P.; Steinke, W. Pharmacokinetics of miglitol. Absorption, distribution, metabolism, and excretion following administration to rats, dogs, and man. *Arzneimittelforschung* **1997**, *47*, 734−745.

(32) Kreymann, B.; Williams, G.; Ghatei, M. A.; Bloom, S. R. Glucagon-like peptide-1 7-36: a physiological incretin in man. *Lancet* **1987**, *2*, 1300−1304.

(33) Zander, M.; Madsbad, S.; Madsen, J. L.; Holst, J. J. Effect of 6-week course of glucagon-like peptide 1 on glycaemic control, insulin sensitivity, and beta-cell function in type 2 diabetes: a parallel-group study. *Lancet* **2002**, *359*, 824−830.

(34) Asano, N.; Ikeda, K.; Yu, Li.; Kato, A.; Takebayashi, K.; Adachi, I.; Kato, I.; Ouchi, H.; Takahata, H.; Fleet, G. W. J. The L-enantiomers of D-sugar-mimicking iminosugars are noncompetitive inhibitors of D-glycohydrolase? *Tetrahedron: Asymmetry* **2005**, *16*, 223−229.

(35) da Cruz, F. P.; Newberry, S.; Jenkinson, S. F.; Wormald, M. R.; Butters, T. D.; Alonzi, D. S.; Nakagawa, S.; Becq, F.; Norez, C.; Nash, R. J.; Kato, A.; Fleet, G. W. J. 4-C-Me-DAB and 4-C-Me-LAB—enantiomeric alkyl-branched pyrrolidine iminosugars—are specific and potent α-glucosidase inhibitors; acetone as the sole protecting group. *Tetrahedron Lett.* **2011**, *52*, 219−223.

(36) Natori, Y.; Imahori, T.; Murakami, K.; Yoshimura, Y.; Nakagawa, S.; Kato, A.; Adachi, I.; Takahata, H. The synthesis and biological evaluation of 1-C-alkyl-L-arabinoiminofuranoses, a novel class of α-glucosidase inhibitors. *Bioorg. Med. Chem. Lett.* **2011**, *21*, 738−741.

(37) Trost, B. M.; Horne, D. B.; Woltering, M. J. Palladium-catalyzed DYKAT of butadiene monoepoxide: enantioselective total synthesis of (+)-DMDP, (−)-bulgecinine, and (+)-broussonetine G. *Chem.—Eur. J.* **2006**, *12*, 6607−6620.

(38) Fu, G. C.; Zhou, J. S. Cross-couplings of unactivated secondary alkyl halides: room-temperature nickel-catalyzed Negishi reactions of alkyl bromides and iodides. *J. Am. Chem. Soc.* **2003**, *125*, 14726−14727.

(39) Phapale, V. B.; Buñuel, E.; García-Iglesias, M.; Cárdenas, D. J. Ni-catalyzed cascade formation of $C(sp^3)$-$C(sp^3)$ bonds by cyclization and cross-coupling reactions of iodoalkanes with alkyl zinc halides. *Angew. Chem., Int. Ed.* **2007**, *46*, 8790−8795.

(40) Calveras, J.; Egido-Gabás, M.; Gómez, L.; Casas, J.; Parella, T.; Joglar, J.; Bujons, J.; Clapés, P. Dihydroxyacetone phosphate aldolase catalyzed synthesis of structurally diverse polyhydroxylated pyrrolidine derivatives and evaluation of their glycosidase inhibitory properties. *Chem.—Eur. J.* **2009**, *15*, 7310−7328.

(41) Best, D.; Jenkinson, S. F.; Saville, A. W.; Alonzi, D. S.; Wormald, M. R.; Butters, T. D.; Norez, C.; Becq, F.; Bleriot, Y.; Adachi, I.; Kato, A.; Fleet, G. W. J. Cystic fibrosis and diabetes: isoLAB and isoDAB, enantiomeric carbon-branched pyrrolidine iminosugars. *Tetrahedron Lett.* **2010**, *51*, 4170−4174.

(42) Scofield, A. M.; Fellows, L. E.; Nash, R. J.; Fleet, G. W. J. Inhibition of mammalian digestive disaccharides by polyhydroxy alkaloids. *Life Sci.* **1986**, *39*, 645−650.

(43) Best, D.; Wang, C.; Weymouth-Wilson, A. C.; Clarkson, R. A.; Wilson, F. X.; Nash, R. J.; Miyauchi, S.; Kato, A.; Fleet, G. W. J. Looking glass inhibitors: scalable syntheses of DNJ, DMDP, and (3R)-3-hydroxy-L-bulgecinine from D-glucuronolactone and of L-DNJ, L-DMDP, and (3S)-3-hydroxy-D-bulgecinine from L-glucuronolactone. DMDP inhibits β-glucosidases and β-galactosidases whereas L-DMDP

is a potent and specific inhibitor of α-glucosidases. *Tetrahedron: Asymmetry* **2010**, *21*, 311−319.

(44) Ellgaard, L.; Molinari, M.; Helenius, A. Setting the standards: quality control in the secretory pathway. *Science* **1999**, *286*, 1882−1888.

(45) Kopito, R. R. ER quality control: the cytoplasmic connection. *Cell* **1997**, *88*, 427−430.

(46) Hammond, C.; Braakman, I.; Helenius, A. Role of N-linked oligosaccharide recognition, glucose trimming, and calnexin in glycoprotein folding and quality control. *Proc. Natl. Acad. Sci. U.S.A.* **1994**, *91*, 913−917.

(47) Hosokawa, N.; Wada, I.; Hasegawa, K.; Yorifuji, T.; Tremblay, L. O.; Herscovics, A.; Nagata, K. A novel ER α-mannosidase-like protein accelerates ER-associated degradation. *EMBO Rep.* **2001**, *2*, 415−422.

(48) Hubbard, S. C.; Ivatt, R. J. Synthesis and processing of asparagines-linked oligosaccharides. *Annu. Rev. Biochem.* **1981**, *50*, 555−583.

(49) Elbein, A. D. Inhibitors of the biosynthesis and processing of N-linked oligosaccharides. *CRC Crit. Rev. Biochem.* **1984**, *16*, 21−49.

(50) Kopito, R. R. ER quality control: the cytoplasmic connection. *Cell* **1997**, *88*, 427−430.

(51) Bonifacino, J. S.; Weissman, A. M. Ubiqitin and the control of protein in the secretory and the endoplasmic pathways. *Annu. Rev. Cell Dev. Biol.* **1998**, *14*, 19−57.

(52) Elbein, A. D. Glycosidase inhibitors: inhibitors of N-linked oligosaccharide processing. *FASEB J.* **1991**, *5*, 3055−3063.

(53) Asano, N.; Oseki, K.; Kizu, H; Matsui, K. Nitrogen-in-the-ring pyranoses and furanoses: structural basis of inhibition of mammalian glycosidases. *J. Med. Chem.* **1994**, *37*, 3701−3706.

(54) Furukawa, J.; Shinohara, Y.; Kuramoto, H.; Miura, Y.; Shimaoka, H.; Kurogochi, M.; Nakano, M.; Nishimura, S. I. Comprehensive approach to structural and functional glycomics based on chemo-selective glycoblotting and sequential tag conversion. *Anal. Chem.* **2008**, *80*, 1094−1101.

(55) Dailey, G. Early and intensive therapy for management of hyperglycemia and cardiovascular risk factors in patients with type 2 diabetes. *Clin. Ther.* **2011**, *33*, 665−678.

(56) Arakawa, M.; Ebato, C.; Mita, T.; Fujitani, Y.; Shimizu, T.; Watada, H.; Kawamori, R.; Hirose, T. Miglitol suppresses the postprandial increase in interleukin 6 and enhances active glucagon-like peptide 1 secretion in viscerally obese subjects. *Metabolism* **2008**, *57*, 1299−1306.

(57) Aoki, K.; Kamiyama, H.; Yoshimura, K.; Shibuya, M.; Masuda, K.; Terauchi, Y. Miglitol administered before breakfast increased plasma active glucagon-like peptide-1 (GLP-1) levels after lunch in patients with type 2 diseases treated with sitagliptin. *Acta Diabetol.* **2012**, *49*, 225−230.

(58) Aguilar-Moncayo, M.; Takai, T.; Higaki, K.; Mena-Barragán, T.; Hirano, Y.; Yura, K.; Li, L.; Yu, Y.; Ninomiya, H.; García-Moreno, M. I.; Ishii, S.; Sakakibara, Y.; Ohno, K.; Nanba, E.; Ortiz Mellet, C.; García Fernández, J. M.; Suzuki, Y. Tuning glycosidase inhibition through aglycone interactions: pharmacological chaperones for Fabry disease and GM1 gangliosidosis. *Chem. Commun.* **2012**, *48*, 6514−6516.

(59) Kato, A.; Yamashita, Y.; Nakagawa, S.; Koike, Y.; Adachi, I.; Hollinshead, J.; Nas, R. J.; Ikeda, K.; Asano, N. 2,5-Dideoxy-2,5-imino-D-aritol as a new class of pharmacological chaperone for Fabry disease. *Bioorg. Med. Chem.* **2010**, *18*, 3790−3794.

(60) Godin, G.; Compain, P.; Masson, G.; Martin, O. R. A general strategy for the practical synthesis of nojirimycin C-glycosides and analogues. Extension to the first reported example of an iminosugar 1-phosphonate. *J. Org. Chem.* **2002**, *67*, 6960−6970.

(61) Godin, G.; Compain, P.; Martin, O. R. General access to iminosugar C-glycoside building blocks by means of cross-metathesis: a gateway to glycoconjugate mimetics. *Org. Lett.* **2003**, *5*, 3269−3272.

(62) Fleet, G. W. J.; Nicholas, S. J.; Smith, P. W.; Evans, S. V.; Fellows, L. E.; Nash, R. J. Potent competitive inhibition of α-galactosidase and α-glucosidase activity by 1,4-dideoxy-1,4-iminopen-titols: synthesis of 1,4-dideoxy-1,4-imino-D-lyxitol and of both enantiomer of 1,4-dideoxy-1,4-iminoarabinitol. *Tetrahedron Lett.* **1985**, *26*, 3127−3130.

(63) Kessler, M.; Acuto, O.; Strelli, C.; Murer, H.; Semenza, G. A. A modified procedure for the rapid preparation of efficiently transporting vesicles from small intestinal brush border membranes. Their use in investigating some properties of D-glucose and choline transport systems. *Biochem. Biophys. Acta* **1978**, *506*, 136−154.

(64) Cooper, C. A.; Gasteiger, E.; Packer, N. GlycoMod—a software tool for determining glycosylation compositions from mass spectro-metric data. *Proteomics* **2001**, *1*, 340−349.

(65) Sim, L.; Willemsma, C.; Mohan, S.; Naim, H. Y.; Pinto, B. M.; Rose, D. R. Structural basis for substrate selectivity in human maltase-glucoamylase and sucrase-isomaltase N-terminal domains. *J. Biol. Chem.* **2010**, *285*, 17763−70.

(66) Laskowski, R. A.; MacArthur, M. W.; Moss, D. S.; Thornton, J. M. PROCHECK: a program to check the stereochemical quality of protein structures. *J. Appl. Crystallogr.* **1993**, *26*, 283−291.

(67) Friesner, R. A.; Banks, J. L.; Murphy, R. B.; Halgren, T. A.; Klicic, J. J.; Mainz, D. T. Glide: a new approach for rapid, accurate docking and scoring. 1. Method and assessment of docking accuracy. *J. Med. Chem.* **2004**, *47*, 1739−1749.

(68) Still, W. C.; Tempczyk, A.; Hawlely, R. C.; Hendrickson, T. Semianalytical treatment of solvation for molecular mechanics and dynamics. *J. Am. Chem. Soc.* **1990**, *112*, 6127−6129.

(69) Sherman, W.; Day, T.; Jacobson, M. P.; Friesner, R. A.; Farid, R. Novel procedure for modeling ligand/receptor induced fit effects. *J. Med. Chem.* **2006**, *49*, 534−553.